***Pak. J. Bot.*, 57(4): DOI: http://dx.doi.org/10.30848/PJB2025-4(40)**

SYSTEMATIC ANALYSIS OF THE bHLH TRANSCRIPTION FACTOR FAMILY IN *TOONA SINENSIS*: POTENTIAL REGULATORY ROLES IN TERPENE SYNTHESIS VIA THE MEP PATHWAY

LIPING REN[1,2], XIANHUI DENG[2], TIANHAO HU[2], MIAO LI[2], WENYANG WAN[2], DANDAN YIN[2], ZONGXIN MA[1] AND XIAOHAN CAO[2*]

[1]Horticultural Institute, Fuyang Academy of Agricultural Sciences, Fuyang, China
[2]Key Laboratory of Horticultural Plant Biology of Biological and Food Engineering School,
Fuyang Normal University, Fuyang236037, Anhui, China
[*]Corresponding author's email: caoxiaohan@163.com

Abstract

Basic helix-loop-helix (bHLH) transcription factors which constitute the second-largest transcription factor superfamily in plants, play an important complex regulatory role in the biosynthesis of plant secondary metabolites. However, little information of bHLH family is available in the multi-prupose horticultural plant *T. sinensis*. Systematic research on the *T. sinensis* bHLH TF family will enable a comprehensive and in-depth understanding of this species. In this study, we identified 132 TsbHLH family members using phylogenetic analysis and categorized them into 21 subfamilies based on their structural characteristics. Then, the bHLH domain, gene structures, protein conserved motifs, cis-regulatory elements and Chromosomal distribution were probed. In addition, we performed a gene duplication analysis and found the TsbHLH TF family is composed of three gene tandems and 96 segmental duplications, which may be responsible for the prosperity of it. Furthermore, 20 differential expressed *TsbHLH* genes identified in a *T. sinensis* transcriptome database were selected to detect their expression across four distinct harvesting periods. Finally, we found that some TsbHLHs may participate in regulating terpene synthesis via the MEP pathway according to the correlation study between the expression of TsbHLHs genes and terpene synthase genes. Our findings provides basic information about TsbHLH TF family and lay a groundwork for further research on the function of *bHLH* genes in regulating the terpene synthesis.

Key words: Toona sinensis; bHLH transcription factors; terpenes; genome-wide analysis; gene expression analysis.

Introduction

Toona sinensis (A. Juss) Roem, a deciduous tree belonging to the Meliaceae family, is indigenous to eastern and southeastern Asia (Dong *et al.*, 2013). *T. sinensis* has been cultivated in China for over 2000 years, due to its timber, medicinal, vegetable and ornamental value (Wang *et al.*, 2022). The tender leaves of *T. sinensis* are highly popular as vegetable owing to its unique aroma, good taste, and rich nutrition (Ren *et al.*, 2021). Research shows terpenes serve an important role in aroma (Ren *et al.*, 2021) and have been experimentally proven to be major component of essential oil from plants (Hyldgaard *et al.*, 2012). In recent years, increasing attention and interests are focused on the diverse value of terpenes. Firstly, essential oils are great food flavorings as natural products (Pandey *et al.*, 2017). Additionally, terpenes possess good antibacterial properties as secondary metabolites, making them suitable for use as food preservatives (Falleh *et al.*, 2020). Furthermore, the essential oil from roots demonstrates its anti-tumour activities through inducing apoptosis of mitochondrial-dependent (Chen *et al.*, 2021). Equally noteworthy, in the seeds of *T. sinensis* , the terpenoids have demonstrated their capacity to mitigate oxidative stress and inflammation induced by high glucose levels in rat glomerular mesangial cells (Chen *et al.*, 2022).

The basic helix-loop-helix (bHLH) family, known for conserved alkaline/helix-loop-helix domains, plays an important role in the biosynthesis of plant secondary metabolites (Feller *et al.*, 2011). The bHLH domain containing approximately 60 amino acids, which has two regions with different functions: a basic region (b) at the N-terminal side and a HLH region at the C-terminal side (Carretero-Paulet *et al.*, 2010). The basic region comprises 13-17 basic amino acids (with a high proportion of basic amino acids) and plays an integral role in binding to the E-box (5'-CANNTG-3') motif within their target genes. On the other hand, the HLH region spans approximately 40-50 amino acids and encompasses two alpha helices demarcated by a variable-length loop. In addition, the HLH region is of great significance due to its important role in dimerization, which is a key process in regulating the expression of target genes involved in different signaling pathways (Massari & Murre, 2000; Nesi *et al.*, 2000). In eukaryotes, *bHLHs* are classified into six main groups (named A, B, C, D, E and F) based on their phylogenetic relationship and DNA binding function (Atchley & Fitch, 1997). To sum up, Group A can specifically bind to the E-box core sequence, while Group B exhibits a preference for binding to the G-box, and Group C displays a binding propensity towards the ACTTG or GCGTG sequence (Henriksson & Lüscher, 1996). Notably, Group D is characterized by the absence of a conventional basic region and primarily engages in heterodimerization with other bHLH family proteins (Sun *et al.*, 1991). In contrast, Group E displays a selective binding inclination towards the CACGNG sequence, whereas members of Group F are proficient in binding to specific DNA target sequences (Fisher & Caudy, 1998; Ledent & Vervoort, 2001).

In 1989, the bHLH genes, TFs E12 and E47 were first discovered in the murine muscle development and since then have been widely studied (Murre *et al.*, 1989). *bHLHs* are found across the genome and present in a wide range of plants, including *Arabidopsis*(Bailey *et al.*, 2003), *Solanum lycopersicum* (Sun *et al.*, 2015), *Cucumis sativus*

(Li *et al.*, 2020b), *Capsicum annuum* (Liu *et al.*, 2021) and *Prunus persica* (Zhang *et al.*, 2018b). It has been proven that bHLH is widely involved in a spectrum of metabolic and developmental processes, such as biosynthesis (Nims *et al.*, 2015; Chu *et al.*, 2018), light signaling (Castelain *et al.*, 2012; Buti *et al.*, 2020), flowering and fruit development (Ito *et al.*, 2012; Yin *et al.*, 2015; Ortolan *et al.*, 2024), and plant morphological development (Zhu *et al.*, 2017; Dong *et al.*, 2018). Additionally, the bHLH family proteins are crucial for resistance to biotic and abiotic stress. Research showed that overexpression of Apple *MdbHLH130* can significantly enhance tolerance to water stress in transgenic Tobacco through regulating stomatal closure and ROS Homeostasis (Zhao *et al.*, 2020). In peanut, overexpression of *AhbHLH121* improves salt tolerance (Zhao *et al.*, 2024).

The maize *R* gene, the first founded member of the bHLH supergene family, has been experimentally confirmed to hold a pivotal role in anthocyanin production (Ludwig *et al.*, 1989). Subsequently, an increasing number of *bHLHs* were shown to regulate secondary metabolic processes in plants. *TcJAMYC*, a bHLH transcription factor in Taxus chinensis, can activates paclitaxel biosynthetic pathway genes (Nims *et al.*, 2015). *PabHLH1* was characterized to regulate the biosynthesis of flavonoids as well as bibenzyls in liverworts and stimulated the accumulation of the flavonols and anthocyanins in *Arabidopsis* (Zhao *et al.*, 2019). It was shown that the bHLH transcription factors Aa6119 and Aa7162 have positive and synergistic effects on the regulation of artemisinin accumulation (Mohammad *et al.*, 2023). Significantly, *bHLHs* has been notably implicated in the regulation of terpenoid biosynthesis. In *Arabidopsis*, *AtMYC2* directly bind to the promoters of sesquiterpene synthase genes *TPS21* and *TPS11*, thereby instigating their expression and concomitantly augmenting sesquiterpene production (Hong *et al.*, 2012). The elevation of terpenoid levels, particularly caryophyllene, was a direct consequence of *LaMYC4* overexpression in Lavender (Dong *et al.*, 2022). Moreover, it was found that in *Taraxacum antungense*, *TaMYC2* plays a positive regulatory role in triterpenoid biosynthesis (Liu *et al.*, 2023). The above studies provide important clues for revealing the molecular mechanism by which bHLH transcription factors regulate terpene synthesis via terpene synthase. Terpenoids, with the most abundant volatile metabolites in plants and significant medicinal value, are synthesized through the cytoplasmic mevalonate (MVA) pathway and the plastid 2-C-methyl-D-erythritol 4-phosphate (MEP) pathway (Vranová *et al.*, 2013). In a singular metabolic cascade, the influence of transcription factors extends to the regulation of a multiplicity of genes. Notably, Several enzyme genes involved in secondary metabolic biosynthesis can have their expression regulated by transcription factors such as WRKY and bHLH in plants (Hong *et al.*, 2012; Ding *et al.*, 2020). However, the existing studies on *T. sinensis* mainly focus on the chemical composition identification of the extracts from different organizations and effects in treating various diseases, little is known about how the synthesis of terpenoids is regulated in *T. sinensis*, especially studies on the regulation of terpene synthesis by bHLH have not been reported yet.

The present study conducted a systemaitic investigation of bHLH TF genes in *T. sinensis.* Here, 132 members of the *TsbHLHs* genes family were identified, and carried out a comprehensive exploration of their physical attributes, subcellular localization, phylogenetic relationships, chromosomal distribution, gene architecture, conserved motifs, and gene promoters. Furthermore, expression patterns of terpene synthase gene and bHLH gene in *Toona sinensis* were analyzed through young leaves at different stages. Our work has established a systematic understanding of the bHLH of Toona sinensis and laid a solid foundation for the subsequent functional research on elucidating the mechanism of regulating terpene biosynthesis.

Material and Methods

Identification of the bHLH transcription factor family of *T. sinensis*: The *T. sinensis* data reported in this study was available under Accession No. CNP0000958 in the CNGB Nucleotide Sequence Archive (CNSA: https://db.cngb.org/search/project/CNP0000958/). In order to identify the *TsbHLH* genes, HMMER 3.0 software was employed with an E-value set at 1e-5, utilizing the Hidden Markov Model (HMM) file of the bHLH domain (ID: PF00010) downloaded from the Pfam database's online search (http://pfam.xfam.org/) (Mistry *et al.*, 2021). The preliminary candidate sequence of *T. sinensis* bHLH was acquired. The total count of conserved structural domains was determined, eliminating incomplete sequences, and retaining members with the bHLH structural domain using the SMART online program (http://smart.embl-heidelberg.de/) and the CCD database (https://www.ncbi.nlm.nih.gov/cdd/) (Lu *et al.*, 2020; Letunic *et al.*, 2021). The online program ExPASy's ProtParam (https://web.expasy.org/protparam/) was utilized to predict the isoelectric point (pI), molecular weights (Mw), amino acid count, Grand Average of Hydropathicity (GRAVY), instability index (II), and aliphatic index (AI) of the identified TsbHLH proteins (Artimo *et al.*, 2012). For forecasting the subcellular positions of TsbHLH proteins, ProtComp 9.0 software from Softberry (http://www.softberry.com) was employed.

Multiple sequence alignment and phylogenetic analysis of the TsbHLHs genes: We used the Clustalw software to align the conserved structural domains of TsbHLH proteins through multiple sequence alignment. Subsequently, the software GeneDoc was employed to manually modify the amino acid sequences of the inferred conserved structural domains. Additionally, all identified TsbHLH genes were classified into distinct categories using the AtbHLH classification system, along with the conserved structural domains of both TsbHLH and AtbHLH proteins (Heim *et al.*, 2003). Employing the Neighbor-Joining (NJ) technique within the MEGA 7.0 program, phylogenetic trees were generated with the settings: p-distance, pairwise deletion, and 1000 bootstrap replicates (Kumar *et al.*, 2016).

Gene structures, protein conserved motifs and Cis-regulatory elements analysis of TsbHLHs genes: The exon-intron structure of the TsbHLHs gene sequence was predicted and visualized using the Gene Structure Display Server (GSDS: http://gsds.gao-lab.org/) (Hu *et al.*, 2015). The MEME online software (http://meme.sdsc.edu/meme/itro.html) was employed to explore the conserved motifs within the identified TsbHLH proteins. The settings used included an "arbitrary" number of repeats, a maximum motif count of "20," a motif width set from 6 to 50, and all other default values (Bailey *et al.*, 2015). For predictive analysis of the Cis-regulatory elements of the genes, the promoter sequence in each TsbHLH (2000 bp upstream of the translation start site) was extracted from the genome and submitted to the PlantCARE online software (http://bioinformatics.psb.ugent.be/webtools/plantcare/html/) (Lescot *et al.*, 2002).

Chromosomal distribution and gene duplication analysis of TsbHLHs genes: Utilizing annotation data from the *T. sinensis* genome, the positioning of *TsbHLHs* on chromosomes was determined. The collinearity among *TsbHLHs* was examined using the Multiple Collinearity Scan Toolkit (MCScanX) program to identify gene duplication events (Wang *et al.*, 2012). The Dual Synteny Plotter software was employed to construct covariance analysis plots comparing *T. sinensis* bHLH genes with those from Arabidopsis, tomato, pineapple, rice, and maize. Genomic data for Arabidopsis, tomato, pineapple, rice, and maize were obtained via Ensembl Plants (http://plants.ensembl.org/index.html).

Plant material and gene expression analysis: The *T. sinensis* var. 'Heiyouchun' utilized was cultivated in a forestry nursery located in Taihe County, Fuyang City, Anhui Province, China in this study. The healthy-growing distal shoots with a minimum of six branches measuring 5 to 10 cm in length from four distinct harvesting periods between March 30 and April 20, 2021, were collected. Each sample was swiftly frozen in liquid nitrogen and stored at -80°C in an ultra-low freezer.

Total RNA was extracted from the specimens following the instructions provided by the Total RNA Extraction Kit (Huayueyang Biotech, Beijing, China). To eliminate any potential genomic DNA contamination, RNase-free DNase I was used. Qualified RNA was identified and selected as the template for first-strand cDNA synthesis through gel electrophoresis and A260/A280 measurements. The cDNA was generated using a reverse transcription kit (Huayueyang Biotech, Beijing, China). Fluorescent quantitative primers with specificity were designed using the Primer Premier 5.0 software based on the sequences of the *TsbHLH* genes and terpene synthase genes. The internal reference gene *TsActin* was employed to quantify expression levels at various harvesting times. The complete primer information is provided in supplemental Table S1. A CFX96 real-time quantitative PCR instrument (Biorad, Los Angeles, CA, USA) was employed for the 25 uL reaction system, as per the instructions of 2×SYBR Green qPCR Mix (With ROX) (Sparkjade, Shandong, China). The reaction procedure comprised the following steps: 94°C for 3 min; 94°C for 20s; 55°C for 20s; 72°C for 30s, repeated for 40 cycles. Each reaction was performed in triplicate for three biological replicates. The $2^{-\Delta\Delta CT}$ method was used to analyze gene expression(Livak & Schmittgen, 2001). For statistical analysis, version 26 of the SPSS software was utilized to calculate the Bonferroni multiple comparisons test. Significant variations between the two groups were defined by average fold changes greater than two and p-values below 0.05.

Results

Identification and physicochemical property analysis of the bHLH gene family members of *T. sinensis*: Based on the conserved domain PF00010 signature file of the bHLH family from the Pfam database, a total of 147 potential bHLH transcription factor sequences were identified in the *T. sinensis* genome database. These potential sequences have been examined using the online tools SMART and CDD to identify conserved structural domains, and those with incomplete structural domains were eliminated. The results are displayed in Table S2. Subsequently, 132 members of the bHLH transcription factors yielded from the complete genome of *T. sinensis* were designated *TsbHLH1* to *TsbHLH132*, based on their positions on the *T. sinensis* chromosome.

A series of physicochemical properties of the *T. sinensis* bHLH proteins were conducted through ExPASy online software, and the main results were as follows: the 132 TsbHLH proteins exhibited molecular weights ranging from 9.8 to 97.1 kD, encoding amino acid varying between 86 and 860, with an average of 384 amino acids. Among them, 80 were categorized as acidic proteins (PI<7), and 52 were identified as basic proteins (PI >7). All proteins exhibited negative GRAVY values which indicates their hydrophilic nature. The analysis of instability index (II) indicated that only 6 TsbHLH proteins were stable (II<40), while the remaining 126 were categorized as unstable (II>40). The aliphatic index (AI) ranged from 49.10 to 109.90. Subcellular localization predictions revealed that 109 TsbHLH proteins were localized in the nucleus, while the remaining 23 TsbHLH proteins were extracellularly localized.

Multiple sequence alignment and phylogenetic analysis of TsbHLHs genes: We used the ClustalW software to carry out the multiple sequence alignments of the conserved structural domains of TsbHLH proteins, and the results revealed that the majority of these domains were approximately 60 amino acids in length. The longest domain comprised 65 amino acids, while the shortest had 54 amino acids (Fig. 1). Within the conserved structural domain of TsbHLH, a total of 31 sites exhibited a higher frequency of conserved amino acids than 50%. Among these, six sites were located in the basic region, nine in the first α-helix, seven in the loop, and nine in the second α-helix. In the two α-helical regions, 95.14% of site 25 and 92.36% of site 63 consisted of hydrophobic amino acid leucine (L). Additionally, 95.83% of sites 16, 22, and 28, and 97.22% of sites 29 and 60 consisted of hydrophobic amino acids (A, F, I, L, M, P, V, W, or Y). Within the basic region of the bHLH structural domain, 116 (81.25%) of the *T. sinensis* bHLH structural domains had glutamate (E) at site 9, with 115 of them also having arginine (R) at site 12.

According to the results of protein sequence alignment between 132 *TsbHLH* and 129 *AtbHLH* genes, a phylogenetic tree was constructed to explore evolutionary relationships within the TsbHLH family. The 132 *TsbHLHs* were categorized into 25 subfamilies based on the *bHLH* gene categorization system in *Arabidopsis,* among them, subfamilies IVc; VI;VIIIa and X exclusively contained *AtbHLH* genes. In other words, the 132 *TsbHLH* genes were divided into 21 subfamilies (Fig. 2). Among these, subfamily Ia held the highest number of *TsbHLH* members (15), followed by subfamilies VIIa and Vb, each with 12 members. Subfamily II had the fewest, comprising only 1 *TsbHLH* gene. The remaining subfamilies contained between 2 and 10 *TsbHLH* genes.

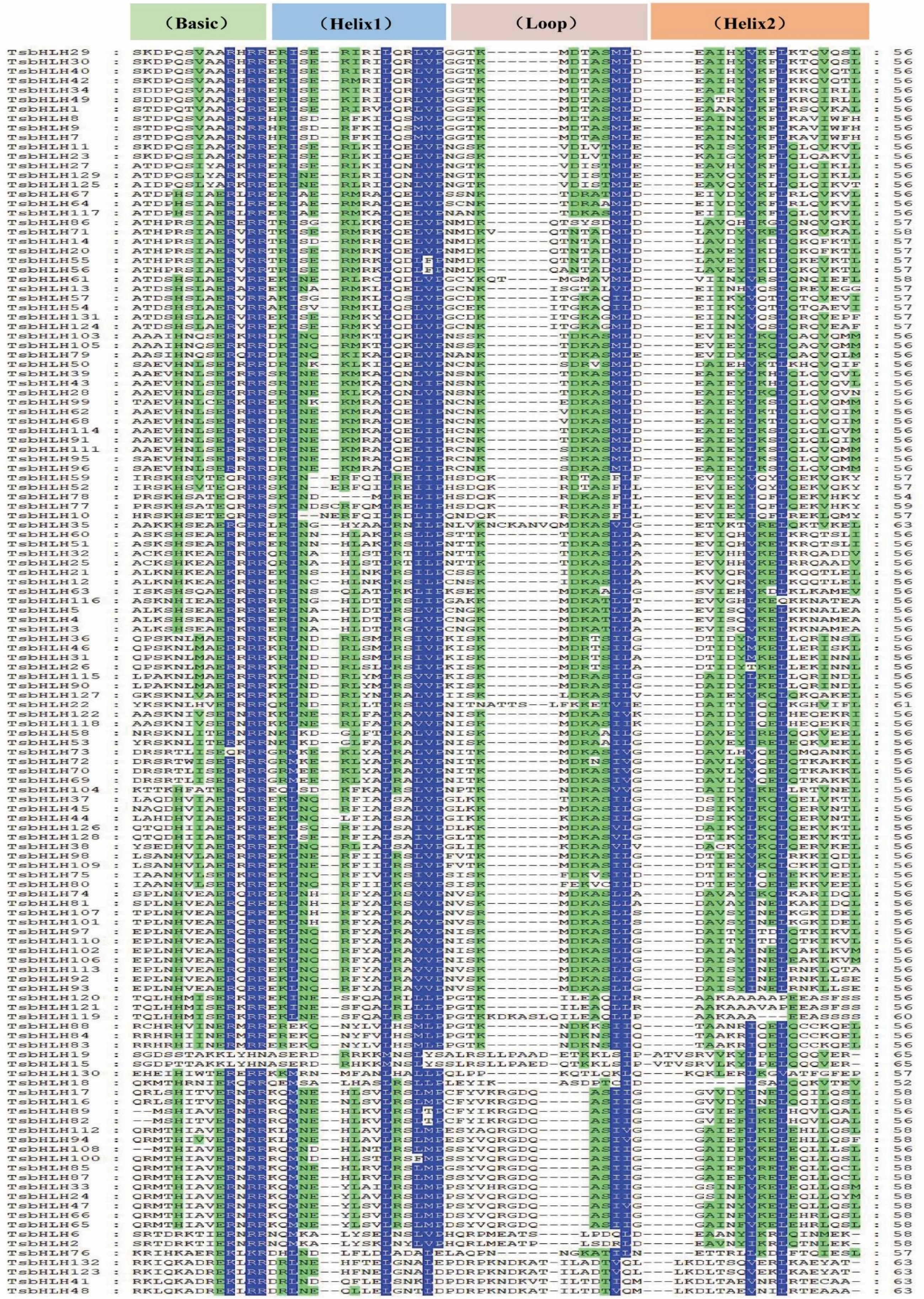

Fig. 1. Multiple sequence alignment of the TsbHLH domains. Amino acids with over 90% identity are highlighted in blue, and those with 50% to 90% identity are marked in red. Dotted lines denote gaps.

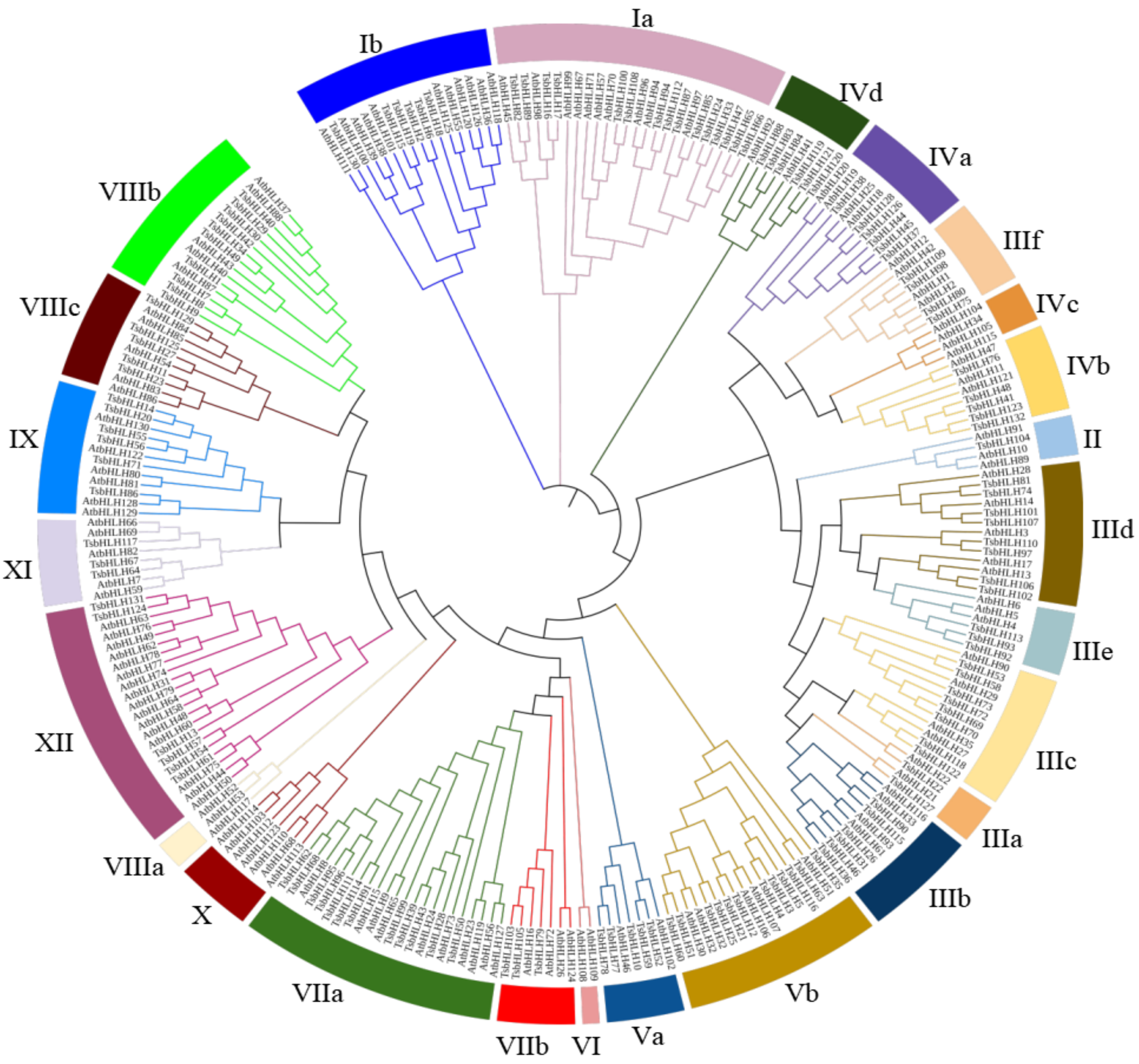

Fig. 2. A phylogenetic tree of bHLH proteins between *T. sinensis* and *A. thaliana*. The tree was constructed using the neighbor-joining (NJ) method with 1,000 bootstrap replications. Different colored arcs represent various groupings of bHLH domains.

Analysis of the gene structure, conserved motifs, and Cis-regulatory elements of TsbHLHs genes: GSDS2.0 software was employed to map the intron-exon structure of *TsbHLHs*. The gene structure results (Fig. 3B) revealed that the exon number of *TsbHLH* genes ranged from 1 to 11, and 89.40% of *TsbHLH* genes contained 1 to 7 exons. Among them, the majority of *TsbHLH* genes (18.18% of the total) had 4 exons. Sixteen *TsbHLH* genes lacked introns, nineteen had only one intron, and these 35 genes were classified into intron deletion group. Interestingly, the members of subfamilies share the same number of introns and exons, while, it varied considerably across distinct subfamilies.

To investigate the structural diversity of the TsbHLH proteins, a statistical analysis of 20 conserved motifs were discovered by utilizing MEME. The result reflects that the TsbHLH protein contains distinct types and numbers of conserved motifs (Fig. 3C). Notably, almost all TsbHLH proteins contain two highly conserved motifs (Motif1 & Motif2), which situated adjacently to each other. Although the length of *TsbHLH* genes varies significantly within the same subfamily, their conserved motifs exhibit similarities in composition and relative positioning. For instance, group Vb contained motifs 1 and 17, group IIIb encompassed motifs 1, 2, and 3, while group XII included motifs 1, 2, and 10.

The PlantCARE online software was employed to explore Cis-regulatory elements within a 2000 bp upstream regulatory (proximal promoter) region extracted from the *TsbHLHs*. Different Cis-regulatory elements were predicted, and the most prevalent were visualized by TBtools program. The results demonstrated (Fig. 4) that the *TsbHLH* genes included a substantial number of promoters' core regulatory elements (TATA-box and CAAT-box), light responsive elements (Box 4, G-Box, G-box, GT1-motif, AE-box, and TCT-motif), and W box elements. We also observed various plant stress response elements, for instance, mechanical injury response elements (WUN-motif), drought-inducible elements (MBS), anaerobic inducible action elements (ARE), low-temperature response elements (LTR and WRE3), and defense and stress response elements (TC-rich repeats). Furthermore, hormone responsive elements were also discovered in *TsbHLH* genes, including abscisic acid response (ABRE),ethylene-responsive elements (ERE), growth hormone-responsive elements (TGA-element), jasmonic acid response (CGTCA-motif and TGACG-motif), salicylic acid response elements (TCA-element), and gibberellin-responsive elements (P-box, TATC-box, and GARE-motif). In this study, all *TsbHLH* genes contained at least one Cis-regulatory element associated with stress response. Elements like ABRE, Box 4, ERE, ARE, and G-box were predicted in over 70% of the *TsbHLH* genes. Some Cis-regulatory elements were found only in a few genes. For example, the TCA-element related to salicylic acid response was present in only 50 *TsbHLH* genes, and the P-box linked to plant gibberellin occurred in only 41 *TsbHLH* genes.

Chromosomal distribution and synteny analysis of TsbHLHs genes: Based on annotation information, we localized the *TsbHLH* genes on *T. sinensis* chromosome (Fig. 5). A total of 132 *TsbHLH* genes were Irregularly and unevenly distributed among the 28 *T. sinensis* chromosome. The Chr23 had the maximum numbers of *TsbHLHs* (14), and secondly, Chr24 contained 13 genes. In contrast, Chr2 and Chr5 respectively held only one *TsbHLH* gene. There were three tandemly duplicated pairs located on Chr11, Chr12 and Chr18 . Moreover, 96 fragment duplication events were identified among the 108 *TsbHLH* genes.

To further explore the evolutionary relationships of the *TsbHLH* genes, we constructed syntenic maps between *T. sinensis* and several representative species (Fig. 6). The representative species included three monocots (pineapple, maize, and rice) and two dicots (*Arabidopsis* and tomato). Syntenic relationships were exhibited between 132 *TsbHLH* genes and those in pineapple (101), Arabidopsis (170), rice (75), tomato (207), and maize (57). Compared to monocots, the *TsbHLH* genes comprised more syntenic gene pairs in dicots.

Expression and correlation analysis of TsbHLHs genes and terpene synthase genes in different harvesting periods: Based on differential expressed genes identified in a *T. sinensis* transcriptome database (unpublished data), 20 *TsbHLH* genes were selected to detect their expression across four distinct harvesting periods. As shown in Fig. 7, expressions of *TsbHLH24* and *TsbHLH33* were down-regulated, while 12 *TsbHLH* genes (7, 13, 15, 75, 91, 94, 97, 103, 108, 112, 124, 131) expression was up-regulated. Interestingly, we noticed that *TsbHLH30* and *TsbHLH4* expressions were first up-regulated, then down-regulated, and then up-regulated. In addition, the other four *TsbHLH* genes were not significantly changed ($|\log2FC| > 1$) in different harvesting periods.

It has been confirmed that several key terpene synthase genes in both the MVA and MEP pathways were significantly changed during the development of *T. sinensis*, with *TsIDI*, *TsDXS*, and *TsDXR* expressions changing over 5-fold(Ren *et al.*, 2022). Figure 8 presents the results of an analysis of gene expression for the remaining *T. sinensis* terpene synthase genes in the MVA and MEP pathways. At diverse harvesting periods, the expression of these genes showed significant changes ($|\log2FC| > 1$). After April 6, all terpene synthase genes except *TsHDR* changed significantly, with *TsMVD*, *TsFPPS*, and *TPS28* expressions changing more than 5-fold during during four different harvesting periods.

The expression of *TsbHLHs* and terpene synthase genes were correlated, and the results are shown in Fig. 9. *TsDXS*, *TsDXR*, *TsHDS*, *TsHDR*, *TsGGPS1* on the MEP pathway, and *TsHMGS* and *TsFPPS1* on the MVA pathway were correlated with some of the *TsbHLH* genes. Additionally, *TsHMGS*, *TsFPPS1*, and *TsbHLH33* have been discovered to be negatively correlated to other genes. While *TsDXS*, *TsHDS*, *TsHDR*, *TsbHLH29*, and *TsbHLH108* were almost all positively correlated factors.

Discussion

The bHLH transcription factors play crucial roles in regulating plant growth and development, stress response, and secondary metabolism (Ito *et al.*, 2012; Zhao *et al.*, 2019; Zhao *et al.*, 2020). In previous studies, we have already known that Terpenoids are the major volatile components of *T. sinensis*,we have also known that *bHLHs* plays an important role in regulating the terpenoid pathway (Qi *et al.*, 2020; Ren *et al.*, 2021). Up to now, extensive studies of the *bHLH* family have been carried out in various plants, such as *Arabidopsis*, rice, and maize (Bailey *et al.*, 2003; Carretero-Paulet *et al.*, 2010; Zhang *et al.*, 2018b). However, the identification and the regulation of terpenoids study of bHLH gene family have never been reported before in *T. sinensis*. For the first time, we have comprehensively identified and analyzed the *bHLH* gene family in *T. sinensis*, which provides important information for revealing the terpene biosynthesis pathway in *T. sinensis*s.

In this study, a total of 132 *TsbHLH* genes were identified. Phylogenic tree analysis indicated that the identified 132 *TsbHLHs* divided into 21 subfamilies. The number of inferred *bHLH* genes in *T. sinensis*s are the same as the number of *bHLH* genes in cucumber (142) (Li *et al.*, 2020b), and greater than some plants such as lotus (115) (Mao *et al.*, 2019), pepper (107) (Liu *et al.*, 2021), and peach (95) (Zhang *et al.*, 2018a), but fewer than in apple (188) (Mao *et al.*, 2017), *Arabidopsis* (162) (Bailey *et al.*, 2003), and tomato (159) (Sun *et al.*, 2015).

The diversity of gene structure is an essential basis for the evolution of gene families, and structural variation plays an important role in the process of gene evolution, in which introns and exons evolve mainly through gain and loss, insertion and deletion (Xu *et al.*, 2012). The *TsbHLH* genes were found to have between 0 and 10 introns, whereas rice (Li *et al.*, 2006) and apple (Yang *et al.*, 2017) had 0 to 5 and 0 to 19 introns, respectively. This finding indicates that the exon-intron of the *bHLH* genes underwent deletion or insertion during the evolution of *T. sinensis*. Most members of the same subfamily share a similar intron-exon distribution, which is the foundation for similar functions amongs members of the same evolutionary group (Li *et al.*, 2020a). Among the 132 TsbHLH proteins, twenty conserved motifs were identified. Conservative motifs within the same subfamily exhibit similarity in composition and relative position. Notably, nearly all TsbHLH proteins contain adjacent Motif1 and Motif2, which together form the bHLH structural domain (Liu *et al.*, 2021). The uniqueness and conservation of conserved motifs of all bHLH proteins in the same subfamily also corroborate the evolutionary classification of the *TsbHLHs* gene family. It is also hypothesized that conserved motifs other than the bHLH structural domain are essential for each subfamily to perform its corresponding function.

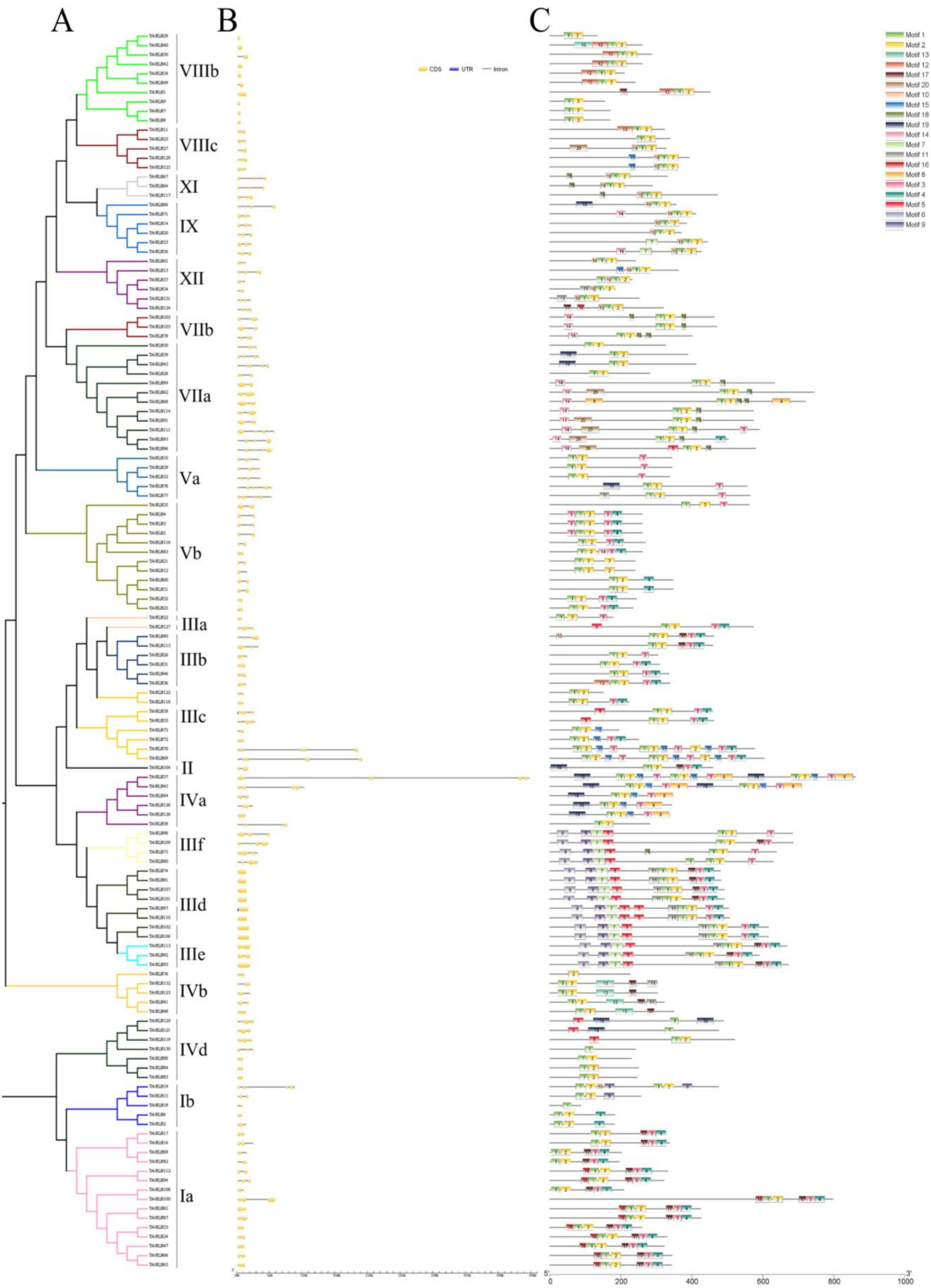

Fig. 3. Phylogenetic tree, exon-intron distribution, and conserved protein motifs of *TsbHLHs*. (A) The *TsbHLHs* are divided into several groups, each with a distinct color. (B) Yellow rectangles and black lines represent exons and introns, respectively. (C) Each motif with conserved amino acid residues is represented in different colors (motifs 1-20).

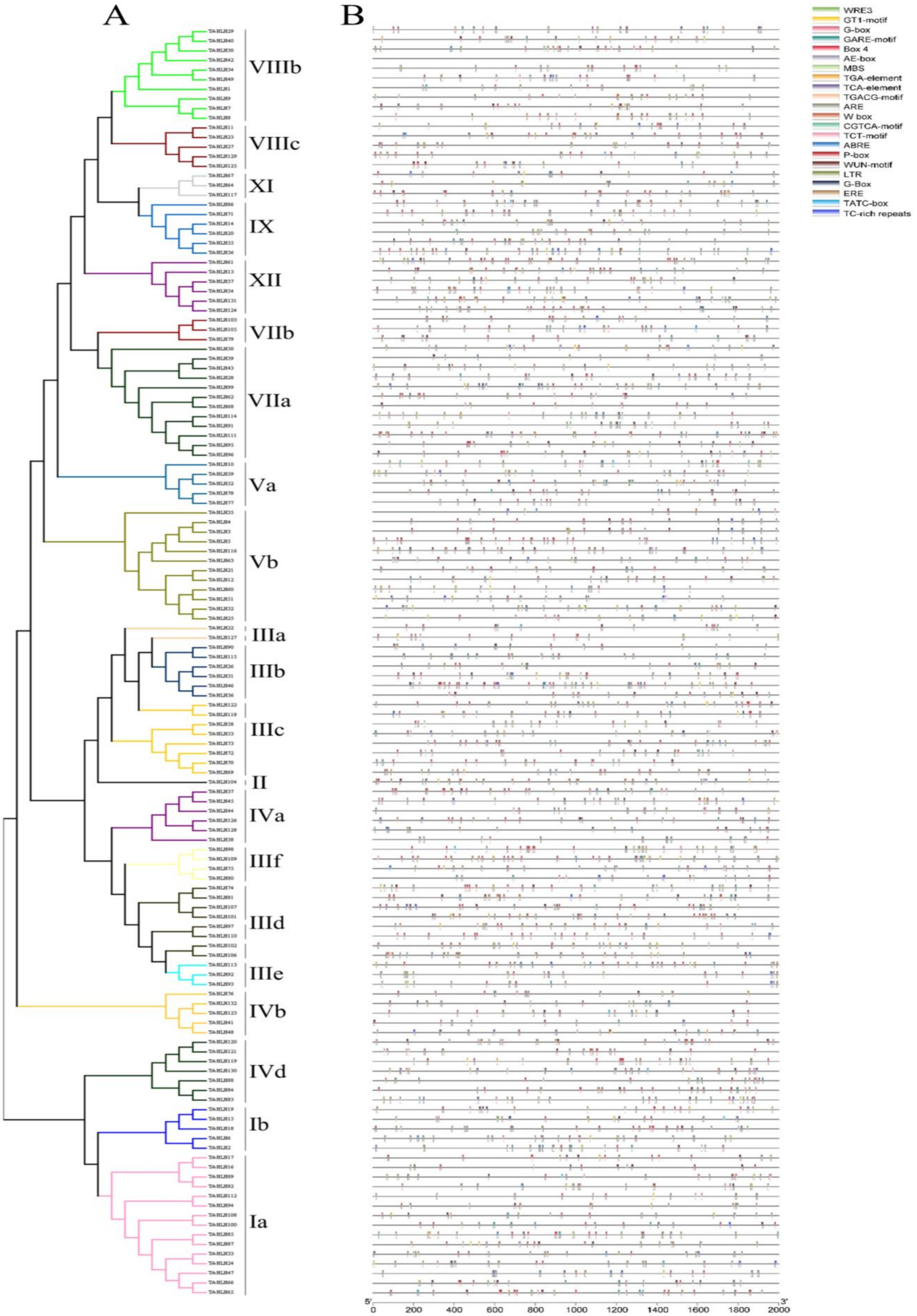

Fig. 4. Prediction of Cis-regulatory elements in the 2000 bp promoter upstream of the *TsbHLHs*. The main Cis-regulatory elements are displayed in the upper right.

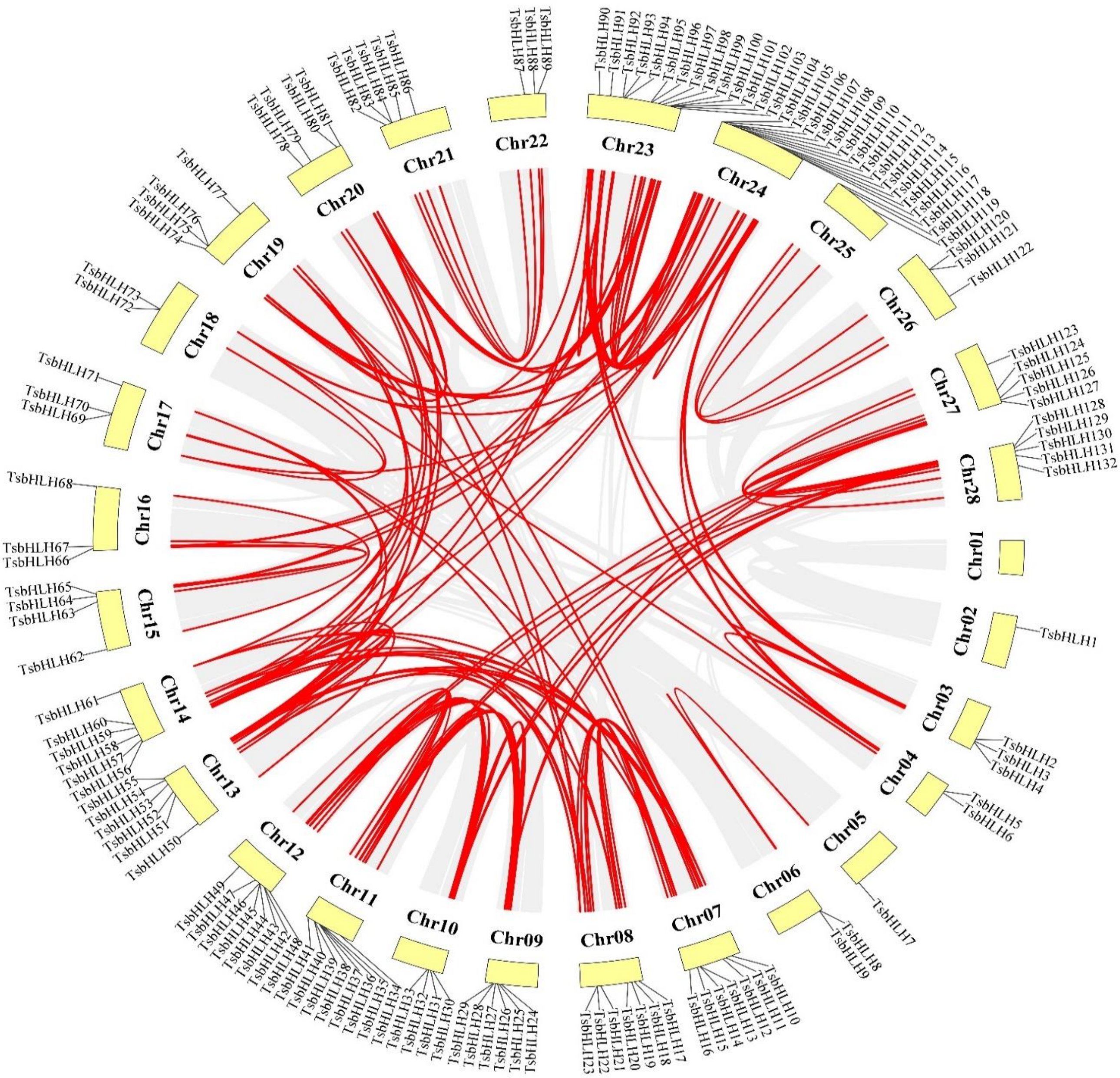

Fig. 5. Segmental duplication of *bHLH* genes in *T.sinensis*. Gray lines indicate synteny blocks, while red lines represent duplicated *bHLH* gene pairs that have been identified.

Genome recombination and amplification are important causes of the diversity of gene family members, and gene duplication usually causes gene recombination and amplification, causing the gene family as a whole to expand (Vision *et al.*, 2000). Gene duplication events include both tandem and fragmental patterns (Cannon *et al.*, 2004). One hundred and thirty-two members of the *T. sinensis* bHLH transcription factor family were irregularly and unevenly distributed on 27 chromosomes, and 96 fragmental duplication events were found in 108 *TsbHLH* genes, along with the presence of three tandem duplication gene pairs, demonstrating that the primary force behind the evolution of the *TsbHLHs* gene family has been fragmental duplication events.

Plant promoters contain many key regulatory elements that respond to gene expression, thereby exerting pivotal regulatory functions at the transcriptional level (Li *et al.*, 2020b). The prediction outcomes of Cis-regulatory elements signify that the promoter sequence of TsbHLH genes comprises an array of coregulatory, hormone-responsive, light-responsive, and stress-responsive elements. It has been demonstrated that plants regulate the expression of stress resistance genes downstream of abiotic stress by means of functional regions within transcription factors that interact with stress-responsive elements (Selvaraj *et al.*, 2020). In a study by Manavella on the sunflower HAHB4 promoter, it was revealed that the ABRE element within the HAHB4 promoter responded to ABA, NaCl, and drought stress (Manavella *et al.*, 2008). Remarkably, 87.88% of *TsbHLH* genes were found to contain ABRE elements, potentially signifying the critical role of *TsbHLH* genes in *T. sinensis*'s response to drought stress. Additionally, the remaining Cis-regulatory elements may be involved in governing plant growth and development while also responding to various abiotic stressors.

Studies have confirmed that terpenoids are the primary volatile components of the Anhui Taihe 'Heiyouchun' cultivar (Liu *et al.*, 2013; Ren *et al.*, 2021). The terpenoids start to be synthesized gradually from sprouting to maturity of *T. sinensis* shoots(Ren *et al.*, 2022). The outcomes of the real-time fluorescence quantitative PCR revealed that 80% of the screened *TsbHLH* genes were significantly different in expression levels at four different harvesting periods. Although the regulatory network of terpenoid synthesis has been less studied, bHLH transcription factors are the main factors in regulating terpenoid metabolism. It is speculated that the accumulation of terpenoids may be connected to the expression of *TsbHLHs*. Thus, the expression patterns of terpene synthase genes on the MVA and MEP pathways were further analyzed and correlated with *TsbHLHs* genes, and several genes on the MEP pathway were found to be involved in the regulation of terpene accumulation. Notably, *TsbHLHs* were highly correlated with the expression trends of 11 terpene synthase genes. For instance, *TsDXS*, *TsDXR*, *TsHDS*, *TsHDR*, *TsbHLH103*, *TsbHLH124*, and *TsbHLH131* may synergistically regulate the synthesis and accumulation of terpenoids.

Transcription factors regulate the transcriptional levels of secondary metabolite synthesis pathway genes. Presently, the primary transcription factors known in relation to terpenoid metabolism include AP2/ERF, WRKY, bHLH, MYC, bZIP, and NAC (Xu *et al.*, 2019). Among these, bHLH transcription factors are chiefly associated with the synthesis of compounds like flavonoids and artemisinin (Qi *et al.*, 2020; Mohammad *et al.*, 2023). The regulatory role of *bHLH* genes involved in plant monoterpenes and sesquiterpenes has yet to be studied, but some research results are available. In *Catharanthus roseus*, *CrMYC2* controls the jasmonate-responsive expression of the ORCA genes that regulate alkaloid biosynthesis(Zhang *et al.*, 2011). *PbbHLH4* overexpression significantly increases the synthesis and accumulation of volatile monoterpenes in Phalaenopsis and significantly increases the aroma of this orchid (Chuang *et al.*, 2018). In tomato (*Solanum lycopersicum*), *SlMYC1* regulates terpene biosynthesis (Xu *et al.*, 2018). In *Litsea cubeba*, overexpression of *LcbHLH78* increased the content of geraniol and linalool (Yang *et al.*, 2022). It was confirmed that *AabHLH112* is a positive regulator of β-stigmasterol, epibasic alcohol and β-farnesene biosynthesis in *Artemisia annua* (Xiang *et al*., 2022). The co-expression network between *TsbHLHs* and a few key genes of terpenoid synthesis provided information to reveal the terpenoid biosynthesis pathway in *T. sinensis*. This study helps to thoroughly investigate the regulatory mechanism of *TsbHLH* in terpene biosynthesis.

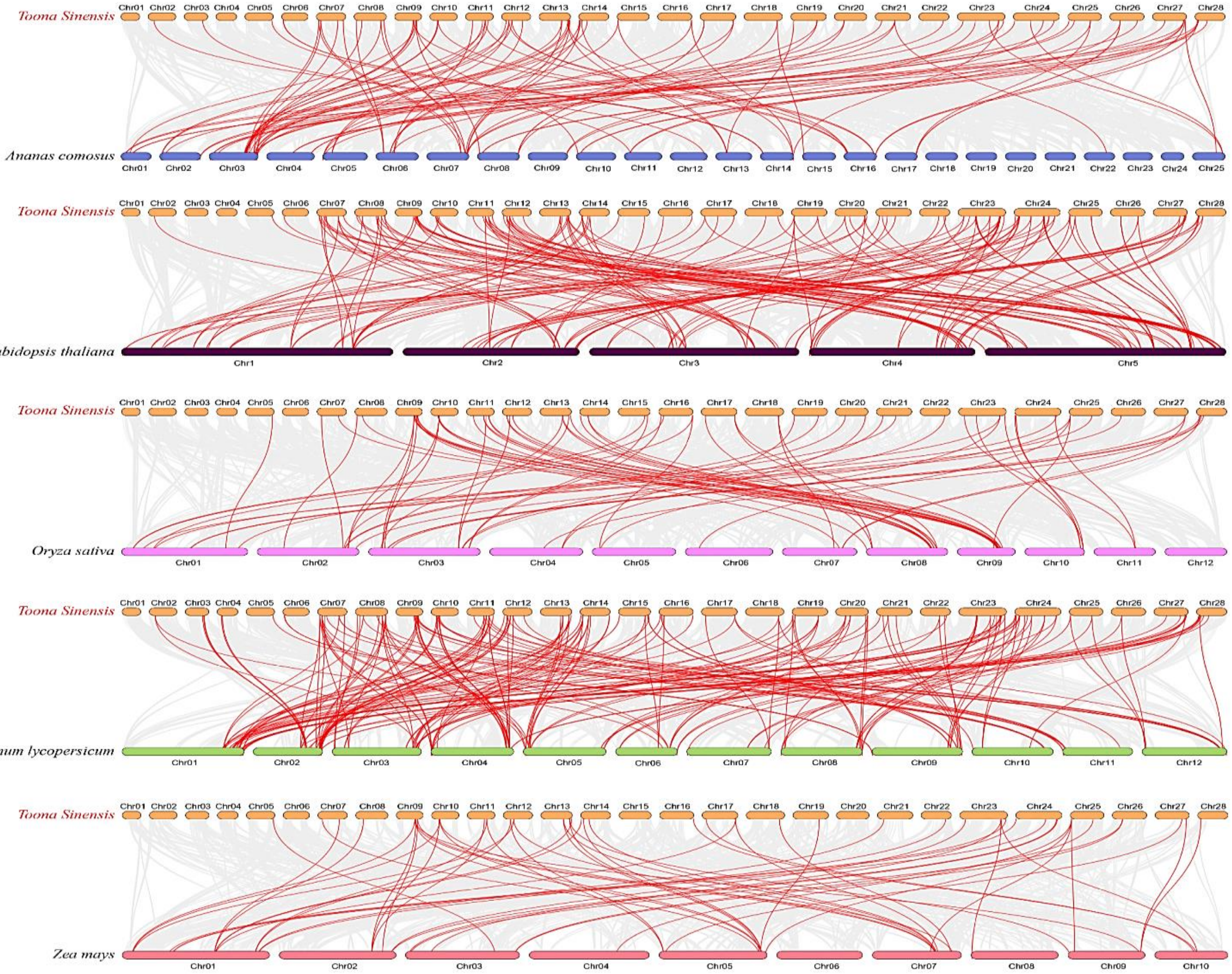

Fig. 6. Synteny analysis of *bHLH* genes between *T. sinensis* and five representative plant species: *Ananas comosus*, *Arabidopsis thaliana*, *Oryza sativa*, *Solanum lycopersicum*, and *Zea mays*. Each horizontal bar signifies a distinct chromosome. Red curves indicate syntenic *bHLH* gene pairs, while gray lines denote collinear blocks within *T. sinensis* and other plant genomes.

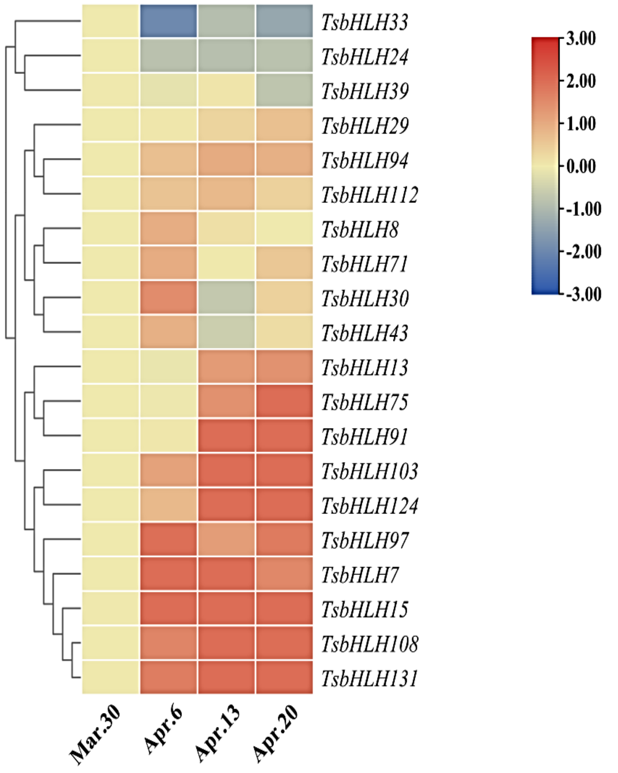

Fig. 7. Differential transcription of *TsbHLHs* genes in four different harvesting periods (March 30, April 6, April 13, and April 20, 2021). Blue and red indicate lower and higher transcript abundance, respectively, compared to the initial data (March 30).

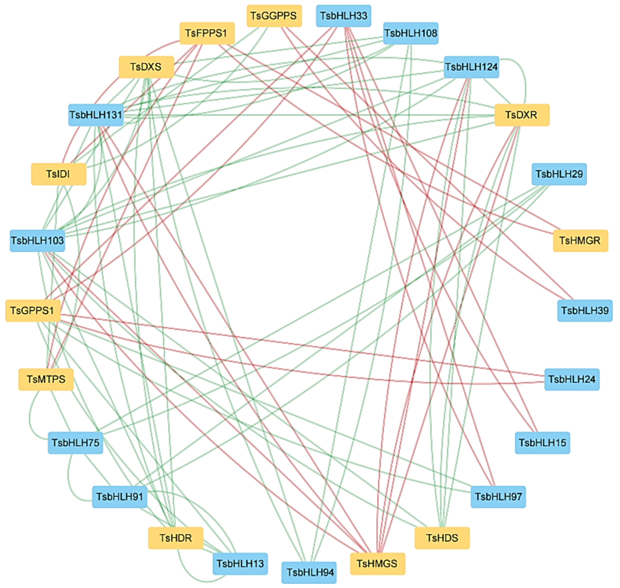

Fig. 9. Correlation analysis of *TsbHLHs* and terpenoid synthesis genes (Pearson correlation coefficient > 0.95). Square nodes colored in blue are *TsbHLHs*, square nodes colored in yellow are terpenoid synthesis genes, green lines represent positive correlation, and red lines represent negative correlation. *HMGS*, 3-hydroxy-3-methylglutaryl-CoA synthase; *HMGR*, 3-hydroxy-3-methylglutaryl-CoA reductase; *IDI*, isopentenyl diphosphate isomerase; *DXS*, 1-deoxyd-xylulose 5-phosphate synthase; *DXR*, 1-deoxy-D-xylulose 5-phosphate reductoisomerase; *GGPPS*, geranylgeranyl diphosphate synthases; *MTPS*, monoterpene synthase.

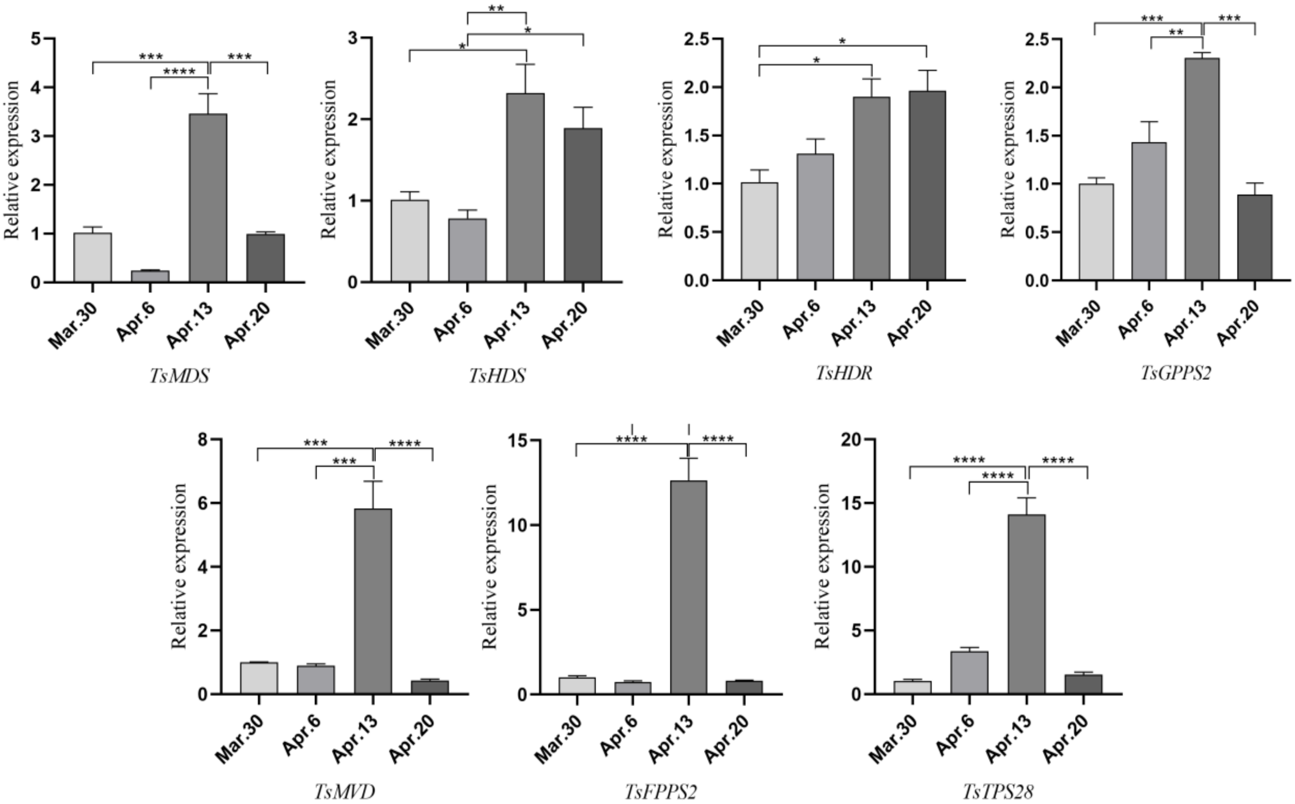

Fig. 8. Expression patterns of several terpene synthase genes in four different harvesting periods (March 30, April 6, April 13, and April 20, 2021). *MDS*, 2-C-methyld-erythritol 2,4-cyclodiphosphate synthase; *HDS*, (E)-4-hydroxy-3-methylbut-2-enyl diphosphate synthase; *HDR*, (E)-4-hydroxy-3-methylbut-2-enyl diphosphate reductase; *GPPS*, Geranylgeranyl pyrophosphate synthase; *MVD*, mevalonate diphosphate decarboxylase; *FPPS*, farnesyl diphosphate synthase; *TPS28*, terpenoid synthase 28. *, **, ***, and **** denote significant differences at p<0.05, p<0.01, p<0.001, and p<0.0001, respectively.

Conclusions

In our study, 132 valid *TsbHLHs* were identified and categorized into 21 subfamilies, all of which possess characteristic HLH domains. The gene structures and conserved motifs within the same subfamily exhibit similarities. *TsbHLH* genes encompass a range of crucial regulatory elements, and some *TsbHLH* genes might participate in regulating terpenoid synthesis via the MEP pathway. The findings of this study contributes to a broad understanding of the bHLH family and lays the foundation for elucidating the mechanism of regulating terpene biosynthesis.

Acknowledgments

This work was supported by the grant from the research funds for postdoctoral researchers in Anhui Province (2020B434), the Natural Science Key Foundations of the Anhui Bureau of Education (KJ2021A0677), the Training Action Project for Young and Middle aged Teachers in universities in Anhui Province (JWFX2023029) and Biological and Medical Sciences of Applied Summit Nurturing Disciplines in Anhui Province (Anhui Education Secretary Department (2023)13).

References

Artimo, P., M. Jonnalagedda, K. Arnold, D. Baratin, G. Csardi, E. de Castro, S. Duvaud, V. Flegel, A. Fortier, E. Gasteiger, A. Grosdidier, C. Hernandez, V. Ioannidis, D. Kuznetsov, R. Liechti, S. Moretti, K. Mostaguir, N. Redaschi, G. Rossier, I. Xenarios and H. Stockinger, 2012. Expasy: Sib bioinformatics resource portal. *Nucl. Acids Res.*, 40(Web Server issue): W597-603.

Atchley, W.R. and W.M. Fitch. 1997. A natural classification of the basic helix-loop-helix class of transcription factors. *Proceedings of the National Academy of Sciences of the United States of America*, 94(10): 5172-5176.

Bailey, P.C., C. Martin, G. Toledo-Ortiz, P.H. Quail, E. Huq, M.A. Heim, M. Jakoby, M. Werber and B. Weisshaar, 2003. Update on the basic helix-loop-helix transcription factor gene family in arabidopsis thaliana. *Plant Cell*, 15(11): 2497-2501.

Bailey, T.L., J. Johnson, C.E. Grant and W.S. Noble. 2015. The meme suite. *Nucl. Acids Res.*, 43(W1): 39-49.

Buti, S., S. Hayes and R. Pierik. 2020. The bhlh network underlying plant shade-avoidance. *Physiol. Plant.*, 169(3): 312-324.

Cannon, S.B., A. Mitra, A. Baumgarten, N.D. Young and G. May. 2004. The roles of segmental and tandem gene duplication in the evolution of large gene families in arabidopsis thaliana. *BMC Plant Biol.*, 4: 10.

Carretero-Paulet, L., A. Galstyan, I. Roig-Villanova, J.F. Martinez-Garcia, J.R. Bilbao-Castro and D.L. Robertson. 2010. Genome-wide classification and evolutionary analysis of the bhlh family of transcription factors in arabidopsis, poplar, rice, moss, and algae. *Plant Physiol.*, 153(3): 1398-1412.

Castelain, M., R. Le Hir and C. Bellini. 2012. The non-DNA-binding bhlh transcription factor pre3/bhlh135/atbs1/tmo7 is involved in the regulation of light signaling pathway in arabidopsis. *Physiol. Plant.*, 145(3): 450-460.

Chen, Y., H. Gao, X. Liu, J. Zhou, Y. Jiang, F. Wang, R. Wang and W. Li. 2022. Terpenoids from the seeds of toona sinensis and their ability to attenuate high glucose-induced oxidative stress and inflammation in rat glomerular mesangial cells. *Molecules (Basel, Switzerland)*, 27(18). DOI 10.3390/molecules27185784.

Chen, Y.C., C.L. Hsieh, B.M. Huang and Y.C. Chen. 2021. Induction of mitochondrial-dependent apoptosis by essential oil of toona sinensis root through akt, mtor and nf-κb signalling pathways in human renal cell carcinoma cells. *J. Food Drug Anal.*, 29(3): 433-447.

Chu, Y., S. Xiao, H. Su, B. Liao, J. Zhang, J. Xu and S. Chen. 2018. Genome-wide characterization and analysis of bhlh transcription factors in panax ginseng. *Acta Pharm. Sinica,* 8(4): 666-677.

Chuang, Y.C., Y.C. Hung, W.C. Tsai, W.H. Chen and H.H. Chen. 2018. Pbbhlh4 regulates floral monoterpene biosynthesis in phalaenopsis orchids. *J. Exp. Bot.*, 69(18): 4363-4377.

Ding, W.J., Q.X. Ouyang, Y.L. Li, T.T. Shi, L. Li, X.L. Yang, K.S. Ji, L.G. Wang and Y.Z. Yue. 2020. Genome-wide investigation of wrky transcription factors in sweet osmanthus and their potential regulation of aroma synthesis. *Tree Physiol.*, 40(4): 557-572.

Dong, H., H. Zhao, S. Li, Z. Han, G. Hu, C. Liu, G. Yang, G. Wang, W. Xie and Y. Xing, 2018. Genome-wide association studies reveal that members of bhlh subfamily 16 share a conserved function in regulating flag leaf angle in rice (*Oryza sativa*). *PLoS Gen.*, 14(4): e1007323.

Dong, X.J., Y.F. Zhu, G.H. Bao, F.L. Hu and G.W. Qin. 2013. New limonoids and a dihydrobenzofuran norlignan from the roots of toona sinensis. *Molecules (Basel, Switzerland)*, 18(3): 2840-2850.

Dong, Y., W. Zhang, J. Li, D. Wang, H. Bai, H. Li and L. Shi. 2022. The transcription factor lamyc4 from lavender regulates volatile terpenoid biosynthesis. *BMC Plant Biol.*, 22(1): 289. DOI 10.1186/s12870-022-03660-3.

Falleh, H., M. Ben Jemaa, M. Saada and R. Ksouri. 2020. Essential oils: A promising eco-friendly food preservative. *Food Chem.*, 330: 127268.

Feller, A., K. Machemer, E.L. Braun and E. Grotewold. 2011. Evolutionary and comparative analysis of myb and bhlh plant transcription factors. *Plant J. Cell & Mol. Biol.*, 66(1): 94-116.

Fisher, A. and M. Caudy. 1998. The function of hairy-related bhlh proteins in cell fate decisions. *BioEssays*, 20: 298-306.

Heim, M.A., J. Marc, W. Martin, M. Cathie, W. Bernd and P.C. Bailey. 2003. The basic helix–loop–helix transcription factor family in plants: A genome-wide study of protein structure and functional diversity. *Mol. Biol. Evol.*, 20(5): 735-747.

Henriksson, M. and B. Lüscher, 1996. Proteins of the myc network: Essential regulators of cell growth and differentiation. *Adv. Cancer Res.*, 68: 109-182.

Hong, G.J., X.Y. Xue, Y.B. Mao and W. Chen. 2012. Arabidopsis myc2 interacts with della proteins in regulating sesquiterpene synthase gene expression. *Plant Cell*, 24(6): 2635-2648.

Hu, B., J.P. Jin, A.Y. Guo, H. Zhang, J.C. Luo and G. Gao. 2015. Gsds 2.0: An upgraded gene feature visualization server. *Bioinformatics*, 31(8): 1296-1297.

Hyldgaard, M., T. Mygind and R.L. Meyer. 2012. Essential oils in food preservation: Mode of action, synergies, and interactions with food matrix components. *Front. Microbiol.*, 3: 12. DOI 10.3389/fmicb.2012.00012.

Ito, S., Y.H. Song, A.R. Josephson-Day, R.J. Miller, G. Breton, R.G. Olmstead and T. Imaizumi. 2012. Flowering bhlh transcriptional activators control expression of the photoperiodic flowering regulator constans in arabidopsis. *Proceed. Nat. Acad. Sci. of the United States of America*, 109: 3582-3587. DOI 10.1073/pnas.1118876109.

Kumar, S., G. Stecher and K. Tamura. 2016. Mega7: Molecular evolutionary genetics analysis version 7.0 for bigger datasets. *Mol. Biol. Evol.*, 33(7): 1870-1874.

Ledent, V. and M. Vervoort. 2001. The basic helix-loop-helix protein family: Comparative genomics and phylogenetic analysis. *Gen. Res.*, 11: 754-770.

Lescot, M., P. Déhais, G. Thijs, K. Marchal, Y. Moreau, Y. Peer, P. Rouzé and S. Rombauts. 2002. Plantcare, a database of plant cis-acting regulatory elements and a portal to tools for in silico analysis of promoter sequences. *Nucl. Acids Res.,* 30(1): 325-327. DOI 10.1093/nar/30.1.325.

Letunic, I., S. Khedkar and P. Bork, 2021. Smart: Recent updates, new developments and status in 2020. *Nucl. Acids Res.*, 49(D1): D458-D460.

Li, H.Y., Y.Z. Yue, W.J. Ding, G.W. Chen, L. Li, Y.L. Li, T.T. Shi, X.L. Yang and L.G. Wang. 2020a. Genome-wide identification, classification, and expression profiling reveals r2r3-myb transcription factors related to monoterpenoid biosynthesis in osmanthus fragrans. *Genes (Basel)*, 11(4): 353. DOI 10.3390/genes11040353.

Li, J., T. Wang, J. Han and Z. Ren. 2020b. Genome-wide identification and characterization of cucumber bhlh family genes and the functional characterization of csbhlh041 in nacl and aba tolerance in arabidopsis and cucumber. *BMC Plant Biol.*, 20(1): 272.

Li, X., X. Duan, H. Jiang, Y. Sun, Y. Tang, Y. Zheng, J. Guo, W. Liang, L. Chen and J. Yin. 2006. Genome-wide analysis of basic/helix-loop-helix transcription factor family in rice and arabidopsis. *Plant Physiol.*, 141(4): 1167.

Liu, C., Z. Jie, Z. Zhou, Z. Hua, H. Wan, Y. Xie, Z. Wang and D. Li. 2013. Analysis of volatile compounds and identification of characteristic aroma components of *toona sinensis* (A. Juss.) roem. Using GC-MS and GC-O. *Food and Nutr. Sci.*, 4(3): 305-314.

Liu, R., J. Song, S. Liu, C. Chen, S. Zhang, J. Wang, Y. Xiao, B. Cao, J. Lei and Z. Zhu. 2021. Genome-wide identification of the capsicum bhlh transcription factor family: Discovery of a candidate regulator involved in the regulation of species-specific bioactive metabolites. *BMC Plant Biol.*, 21(1): 262. DOI 10.1186/s12870-021-03004-7.

Liu, T., J. Liao, M. Shi, L. Li, Q. Liu, X. Cui, W. Ning and G. Kai. 2023. A jasmonate-responsive bhlh transcription factor tamyc2 positively regulates triterpenes biosynthesis in taraxacum antungense kitag. *Plant Sci.*, 326: 111506.

Livak, K.J. and T.D. Schmittgen. 2001. Analysis of relative gene expression data using real-time quantitative PCR and the 2(-delta delta c(t)) method. *Methods*, 25(4): 402-408.

Lu, S., J. Wang, F. Chitsaz, M.K. Derbyshire, R.C. Geer, N.R. Gonzales, M. Gwadz, D.I. Hurwitz, G.H. Marchler, J.S. Song, N. Thanki, R.A. Yamashita, M. Yang, D. Zhang, C. Zheng, C.J. Lanczycki and A. Marchler-Bauer. 2020. Cdd/sparcle: The conserved domain database in 2020. *Nucl. Acids Res.*, 48(D1): D265-D268.

Ludwig, S.R., L.F. Habera, S.L. Dellaporta and S.R. Wessler. 1989. Lc, a member of the maize r gene family responsible for tissue-specific anthocyanin production, encodes a protein similar to transcriptional activators and contains the myc-homology region. *Proceed. Nat. Acad. Sci. of the United States of America*, 86(18): 7092-7096.

Manavella, P.A., C.A. Dezar, F.D. Ariel and R.L. Chan. 2008. Two abres, two redundant root-specific and one w-box cis-acting elements are functional in the sunflower hahb4 promoter. *Plant Physiol. Biochem.*, 46(10): 860-867.

Mao, K., Q.L. Dong, C. Li, C.H. Liu and F.W. Ma. 2017. Genome wide identification and characterization of apple bhlh transcription factors and expression analysis in response to drought and salt stress. *Front. Plant Sci.*, 8: 480. DOI 10.3389/fpls.2017.00480.

Mao, T., Y, Y. Liu, Y, H. Zhu, H, J. Zhang and J. Yang. 2019. Genome-wide analyses of the bhlh gene family reveals structural and functional characteristics in the aquatic plant nelumbo nucifera. *Peer J.*, 7: e7153.

Massari, M.E. and C. Murre. 2000. Helix-loop-helix proteins: Regulators of transcription in eucaryotic organisms. *Mol. Cell. Biol.*, 20(2): 429-440.

Mistry, J., S. Chuguransky, L. Williams, M. Qureshi, G.A. Salazar, E.L.L. Sonnhammer, S.C.E. Tosatto, L. Paladin, S. Raj, L.J. Richardson, R.D. Finn and A. Bateman, 2021. Pfam: The protein families database in 2021. *Nucl. Acids Res.*, 49(D1): D412-D419.

Mohammad, I.M. Hurrah, A. Kumar and N. Abbas. 2023. Synergistic interaction of two bhlh transcription factors positively regulates artemisinin biosynthetic pathway in *Artemisia annua* L. *Physiol. Plant.*, 175(1): e13849.

Murre, C., P.S. McCaw and D. Baltimore. 1989. A new DNA binding and dimerization motif in immunoglobulin enhancer binding, daughterless, myod, and myc proteins. *Cell*, 56: 777-783.

Nesi, N., I. Debeaujon, C. Jond, G. Pelletier and L. Lepiniec. 2000. The tt8 gene encodes a basic helix-loop-helix domain protein required for expression of dfr and ban genes in arabidopsis siliques. *The Plant Cell*, 12(10): 1863-1878.

Nims, E., K. Vongpaseuth, S.C. Roberts and E.L. Walker. 2015. Tcjamyc: A bhlh transcription factor that activates paclitaxel biosynthetic pathway genes in yew. *J. Biol. Chem.*, 290(33): 20104. DOI 10.1074/jbc.A109.026195.

Ortolan, F., T.S. Trenz, C.L. Delaix, F. Lazzarotto and M. Margis-Pinheiro. 2024. Bhlh-regulated routes in anther development in rice and arabidopsis. *Gen. Mol. Biol.*, 46(3 Suppl 1): e20230171.

Pandey, A.K., P. Kumar, P. Singh, N.N. Tripathi and V.K. Bajpai. 2017. Essential oils: Sources of antimicrobials and food preservatives. *Front. Microbiol.*, 7: 2161. DOI 10.3389/fmicb.2016.02161.

Qi, Y., L. Zhou, L. Han, H.Z. Zou, K. Miao and Y. Wang. 2020. Psbhlh1, a novel transcription factor involved in regulating anthocyanin biosynthesis in tree peony (*Paeonia suffruticosa*). *Plant Physiol. Biochem*, 154: 396-408.

Ren, L.P., W.Y. Wan, Y.H. Xie, B.B. Chen, G.S. Wang, D.D. Yin, X.H. Su and X.H. Cao. 2021. Identification of volatile aroma compounds of toona sinensis (a. Juss) roem buds and investigation of genes expression profiles confering aroma production. *Pak. J. Bot.*, 53(4): 1459-1464.

Ren, L.P., W.Y. Wan, D.D. Yin, X.H. Deng, Z.X. Ma, T. Gao and X.H. Cao. 2022. Genome-wide analysis of wrky transcription factor genes in toona sinensis: An insight into evolutionary characteristics and terpene synthesis. *Front. Plant Sci.*, 13: 1063850. DOI 10.3389/fpls.2022.1063850.

Selvaraj, M.G., A. Jan, T. Ishizaki, M. Valencia, B. Dedicova, K. Maruyama, T. Ogata, D. Todaka, K. Yamaguchi-Shinozaki, K. Nakashima and M. Ishitani. 2020. Expression of the ccch-tandem zinc finger protein gene ostzf5 under a stress-inducible promoter mitigates the effect of drought stress on rice grain yield under field conditions. *Plant Biotech. J.*, 18(8): 1711-1721.

Sun, H., H.J. Fan and H.Q. Ling. 2015. Genome-wide identification and characterization of the bhlh gene family in tomato. *BMC Genom.*, 16(1): 9.

Sun, X.H., N.G. Copeland, N.A. Jenkins and D. Baltimore. 1991. Id proteins id1 and id2 selectively inhibit DNA binding by one class of helix-loop-helix proteins. *Mol. Cell. Biol.*, 11(11): 5603-5611.

Vision, T.J., D.G. Brown and S.D. Tanksley. 2000. The origins of genomic duplications in arabidopsis. *Science*, 290(5499): 2114-2117.

Vranová, E., D. Coman and W. Gruissem. 2013. Network analysis of the mva and mep pathways for isoprenoid synthesis. *Ann. Rev. Plant Biol.*, 64: 665-700.

Wang, X., Y. Xiao, Z.H. He, L.L. Li, Y.W. Lv and X.S. Hu. 2022. Evolutionary divergence between toona ciliata and toona sinensis assayed with their whole genome sequences. *Genes (Basel)*, 13(10): 1799. DOI 10.3390/genes13101799.

Wang, Y.P., H.B. Tang, J.D. Debarry, X. Tan, J.P. Li, X.Y. Wang, T.H. Lee, H.Z. Jin, B. Marler, H. Guo, J.C. Kissinger and A.H. Paterson. 2012. Mcscanx: A toolkit for detection and evolutionary analysis of gene synteny and collinearity. *Nucl. Acids Res.*, 40(7): e49. DOI 10.1093/nar/gkr1293.

Xiang, L., P. He, G. Shu, M. Yuan, M. Wen, X. Lan, Z. Liao and Y. Tang. 2022. Aabhlh112, a bhlh transcription factor, positively regulates sesquiterpenes biosynthesis in artemisia annua. *Front. Plant Sci.*, 13: 973591.

Xu, G., C.C. Guo, H.Y. Shan and H.Z. Kong. 2012. Divergence of duplicate genes in exon-intron structure. *Proceed. Nat. Acad. Sci. of the United States of America*, 109(4): 1187-1192.

Xu, J., Z.O. van Herwijnen, D.B. Dräger, C. Sui, M.A. Haring and R.C. Schuurink. 2018. Slmyc1 regulates type vi glandular trichome formation and terpene biosynthesis in tomato glandular cells. *Plant Cell*, 30(12): 2988-3005.

Xu, Y., C. Zhu, C. Xu, J. Sun and K. Chen. 2019. Integration of metabolite profiling and transcriptome analysis reveals genes related to volatile terpenoid metabolism in finger citron (c. Medica var. Sarcodactylis). *Molecules (Basel, Switzerland)*, 24(14): 2564.

Yang, J., Y. Chen, M. Gao, L. Wu, S. Xiong, S. Wang, J. Gao, Y. Zhao and Y. Wang. 2022. Comprehensive identification of bhlh transcription factors in litsea cubeba reveals candidate gene involved in the monoterpene biosynthesis pathway. *Front. Plant Sci.*, 13: 1081335.

Yang, J., M. Gao, L. Huang, Y. Wang and H. Gao. 2017. Identification and expression analysis of the apple (malus × domestica) basic helix-loop-helix transcription factor family. *Sci. Reports*, 7(1): 28. DOI 10.1038/s41598-017-00040-y.

Yin, J., X. Chang, T. Kasuga, M. Bui, M.S. Reid and C.Z. Jiang. 2015. A basic helix-loop-helix transcription factor, phfbh4, regulates flower senescence by modulating ethylene biosynthesis pathway in petunia. *Hort. Res.*, 2: 15059.

Zhang, C.H., R.C. Feng, R.J. Ma, Z.J. Shen, Z.X. Cai, Z.Z. Song, B. Peng and M.L. Yu. 2018a. Genome-wide analysis of basic helix-loop-helix superfamily members in peach. *PLoS One*, 13(4): e0195974.

Zhang, H., S. Hedhili, G. Montiel, Y. Zhang, G. Chatel, M. Pré, P. Gantet and J. Memelink. 2011. The basic helix-loop-helix transcription factor crmyc2 controls the jasmonate-responsive expression of the orca genes that regulate alkaloid biosynthesis in catharanthus roseus. *Plant J*, 67(1): 61-71.

Zhang, T., W. Lv, H. Zhang, L. Ma, P. Li, L. Ge and G. Li. 2018b. Genome-wide analysis of the basic helix-loop-helix (bhlh) transcription factor family in maize. *BMC Plant Biol.*, 18(1): 235.

Zhao, Q., Z. Fan, L. Qiu, Q. Che and Y. Wang. 2020. Mdbhlh130, an apple bhlh transcription factor, confers water stress resistance by regulating stomatal closure and ros homeostasis in transgenic tobacco. *Front. Plant Sci.*, 11: 543696.

Zhao, X., Q. Wang, C. Yan, Q. Sun, J. Wang, C. Li, C. Yuan, Y. Mou and S. Shan. 2024. The bhlh transcription factor ahbhlh121 improves salt tolerance in peanut. *Int. J. Biol. Macromol.*, 256: 128492.

Zhao, Y., Y.Y. Zhang, H. Liu, X.S. Zhang, R. Ni, P.Y. Wang, S. Gao, H.X. Lou and A.X. Cheng. 2019. Functional characterization of a liverworts bhlh transcription factor involved in the regulation of bisbibenzyls and flavonoids biosynthesis. *BMC Plant Biol.*, 19(1): 497. DOI 10.1186/s12870-019-2109-z.

Zhu, Z., G. Chen, X. Guo, W. Yin, X. Yu, J. Hu and Z. Hu. 2017. Overexpression of slpre2, an atypical bhlh transcription factor, affects plant morphology and fruit pigment accumulation in tomato. *Sci. Reports*, 7(1): 5786.

(Received for publication 11 August 2024)

Table S1. Primers used in RT-qPCR.

Gene	Forward Primer (5'-3')	Reverse Primer (5'-3')
TsbHLH7	CTTCCGGGTTCTTTTCCTTA	TCTTCACTTTGGAAGCCATT
TsbHLH8	ATCCGTAGCATCCCTTCC	TTAATGCGTCTGACTCTTCATC
TsbHLH13	CACGTATGAAGCTGCTACAAGA	CAGGGAAGTTACCGTCCATTA
TsbHLH15	AAGAAACTAAGCATTCCGGT	TGACAAAAGCTGTTCCTTCT
TsbHLH24	TTTACTCTTTGGGAGGAGGA	GCATGTTGAATCACTGAAGG
TsbHLH29	ATGGACACTGCCTCTATGTT	TGCTGACCGTTTTGAACT
TsbHLH30	CCACCAAGGAGAAGAAATGT	CAGGGACAAGTCTTTGAAGT
TsbHLH33	TCACGAAGAAACGACCCA	TTCCTCGACCTGCTTAACAC
TsbHLH39	TCTCAGATGACAACGGGATT	ATACTTGGCACATTGGGTAG
TsbHLH43	AAGGCTCTGATCGAAAGG	CAAGTGCGGGGAAAGTAT
TsbHLH71	CCACCAAAAACAGATGAACC	TTTCTGGACTTGAAGGTCTG
TsbHLH75	GCGAAGGGAAAAGCTAAATC	GTCTCTAACTCTGCTCTGTG
TsbHLH91	CAAAGAAATACAATGCCTCC	GTCCCTTACAAGATCCTAACTCAC
TsbHLH94	ACCTCCTTTTTCCCAGTTTT	GAAGTTTTGCATGGGTTTCA
TsbHLH97	GCATAAACAGATTCCAGTGC	GTCCTCCGTTGTAGAAACAT
TsbHLH103	AACTCCAGATGTCGATGATG	CACGCTAGGAATGTGGATAA
TsbHLH108	CAGTTGTTGAAAGCCATTGT	AATGTTCTGTTCCCCTTCTC
TsbHLH112	ATCCTTTCTCGACGAAGT	ACTGATAGAGTAGAGGACCAAT
TsbHLH124	AATCCTGCCTACCTTCCTTT	TGGTTCTCCTTAGCCCAATA
TsbHLH131	TCAGATATTGGGCTAAGGAGA	TGAGATGGAAAGTGCGTTG
TsMVD	GAAGGACTGGGAAAAATTGC	GCTGGCTCTGATTTTCTTTC
TsMDS	AAGCTATCAGAACCAACCTG	TGAGCTGCAATACTTCGATT
TsHDR	GGAACTCAAGCAATACCTCA	TTCTTTCTCAACCAGCTCTC
TsHDS	ATATTGACGCTACGATGCTT	ATGGTGAATTACAGGCAAGT
TsFPPS2	CTCTTAGCCTTGCTCATTCA	TGACAGGCTAAAACCTTCTC
TsGPPS2	GCTGTTGTTTCAGGTAGTTG	CTTTGATCCTTCAATCCCCA
TsTPS28	TAAGACAGCAGTCTTGGTG	CAATTTACATACCTTCCGT
TsActin1	TATGGTTGGTATGGGTCAGA	GTGTGATGCCAGATTTTCTC

Table S2. The physiological and biochemical properties of bHLH genes in *T. sinensis*.

Gene name	Gene locus	Chromosome location	Subcellular localization	pI	Mw (Da)	Protein length	GRAVY	Instability index	Aliphatic index
TsbHLH1	Maker00019392	Chr02 (3910161..3911600)	Nuclear	5.22	49778.15	451	-0.64	53.62	72.26
TsbHLH2	Maker00018298	Chr03 (12608021..12609255)	Extracellular	9.24	20344.24	181	-0.502	36.48	83.54
TsbHLH3	Maker00018229	Chr03 (13365638..13368390)	Nuclear	8.26	28467.38	259	-0.363	43.65	81.81
TsbHLH4	Maker00022311	Chr03 (13746914..13749664)	Nuclear	8.26	28419.33	259	-0.358	43.65	82.93
TsbHLH5	Maker00012521	Chr04 (2718559..2721307)	Nuclear	8.95	28382.36	259	-0.335	47.58	84.05
TsbHLH6	Maker00021798	Chr04 (3403637..3404407)	Extracellular	7.93	20513.37	182	-0.521	38.23	79.34
TsbHLH7	Maker00011935	Chr05 (18312734..18313243)	Nuclear	5.72	19078.18	169	-0.714	62.47	58.28
TsbHLH8	Maker00009754	Chr06 (943523..944029)	Nuclear	5.16	19021.00	168	-0.704	66.81	58.04
TsbHLH9	Maker00019102	Chr06 (1115512..1115973)	Nuclear	9.47	17144.24	153	-0.51	52.21	66.93
TsbHLH10	Maker00034188	Chr07 (3203694..3207203)	Nuclear	5.36	38276.24	343	-0.84	58.81	62.83
TsbHLH11	Maker00005037	Chr07 (5156279..5157584)	Nuclear	6.10	35905.70	322	-0.758	38.28	60
TsbHLH12	Maker00010518	Chr07 (6238020..6239480)	Nuclear	8.17	27101.00	239	-0.436	54.47	89.37
TsbHLH13	Maker00025107	Chr07 (14531686..14535508)	Nuclear	6.28	39657.63	361	-0.863	52.55	66.23
TsbHLH14	Maker00025042	Chr07 (14583598..14585845)	Nuclear	8.59	42578.41	384	-0.621	55.17	65.23
TsbHLH15	Maker00025000	Chr07 (15583769..15585508)	Nuclear	6.19	29379.29	255	-0.467	60.26	89.1
TsbHLH16	Maker00004958	Chr07 (18294797..18297282)	Nuclear	5.34	36970.60	336	-0.39	58.72	86.16
TsbHLH17	Maker00018660	Chr08 (1410441..1411554)	Nuclear	5.32	35689.04	326	-0.425	56.41	86.41
TsbHLH18	Maker00003964	Chr08 (2992953..2993752)	Nuclear	9.46	9787.06	86	-1.009	64.05	74.88
TsbHLH19	Maker00003886	Chr08 (3922562..3931692)	Extracellular	8.56	54229.97	474	-0.486	67.92	89.94
TsbHLH20	Maker00031426	Chr08 (5153458..5155842)	Nuclear	8.63	40975.37	370	-0.77	47.66	57.97
TsbHLH21	Maker00032321	Chr08 (14720168..14721560)	Nuclear	7.73	27164.00	239	-0.456	61.17	90.17
TsbHLH22	Maker00003302	Chr08 (15819709..15820392)	Extracellular	9.16	20223.53	177	-0.462	45.57	95.76
TsbHLH23	Maker00003348	Chr08 (15856264..15857623)	Nuclear	6.67	37347.53	337	-0.689	32.74	68.07
TsbHLH24	Maker00008404	Chr09 (12661277..12662499)	Nuclear	5.69	36631.09	329	-0.539	59.78	73.53
TsbHLH25	Maker00006272	Chr09 (13355995..13356784)	Nuclear	6.54	25940.98	233	-0.68	48.11	66.57
TsbHLH26	Maker00006155	Chr09 (13898548..13900118)	Nuclear	4.95	34917.58	304	-0.506	53.19	73.75
TsbHLH27	Maker00005958	Chr09 (14599184..14600697)	Nuclear	4.54	36071.11	326	-0.471	55.15	69.69
TsbHLH28	Maker00006073	Chr09 (15079607..15082096)	Extracellular	6.10	30509.88	281	-0.508	60.81	72.21
TsbHLH29	Maker00006030	Chr09 (15166082..15166480)	Nuclear	10.26	14846.17	132	-0.536	55.86	81.36
TsbHLH30	Maker00005722	Chr10 (3566828..3568539)	Nuclear	6.93	31799.00	285	-0.571	49.15	65.44
TsbHLH31	Maker00005696	Chr10 (4351996..4353218)	Nuclear	4.69	35024.60	308	-0.467	63.54	75.71
TsbHLH32	Maker00007903	Chr10 (5007017..5007841)	Nuclear	5.92	26943.29	243	-0.56	49.81	71.4
TsbHLH33	Maker00007936	Chr10 (5448552..5449549)	Nuclear	7.06	28946.65	259	-0.55	68.81	74.21
TsbHLH34	Maker00013999	Chr11 (4668602..4669231)	Nuclear	5.76	23922.89	209	-0.8	63.4	73.73
TsbHLH35	Maker00032680	Chr11 (11419547..11422205)	Extracellular	8.83	62692.89	561	-0.753	33.85	71.52
TsbHLH36	Maker00009621	Chr11 (12840940..12842295)	Nuclear	5.15	38242.18	337	-0.539	59.87	76.38
TsbHLH37	Maker00009677	Chr11 (13084232..13130481)	Extracellular	8.61	97057.52	860	-0.495	57.11	84.48
TsbHLH38	Maker00009594	Chr11 (13137339..13145223)	Extracellular	8.51	32373.75	281	-0.189	51.65	107.19
TsbHLH39	Maker00020140	Chr11 (14985457..14988879)	Extracellular	5.63	42204.79	387	-0.504	52.2	72.27
TsbHLH40	Maker00020154	Chr11 (15053064..15053843)	Nuclear	9.54	28894.38	259	-0.447	61.2	64.4
TsbHLH41	Maker00031833	Chr11 (17612619..17614397)	Nuclear	6.03	36075.86	321	-1.035	52.97	57.69
TsbHLH42	Maker00026700	Chr12 (2955273..2956052)	Nuclear	9.32	28874.46	259	-0.412	57.13	65.52
TsbHLH43	Maker00026395	Chr12 (3018505..3023506)	Extracellular	5.94	44988.61	411	-0.624	59.41	68.3
TsbHLH44	Maker00026830	Chr12 (4884276..4886049)	Nuclear	5.74	38932.10	346	-0.382	58.12	88.76
TsbHLH45	Maker00026825	Chr12 (4906191..4916772)	Extracellular	6.90	78720.20	709	-0.385	55.55	86.08
TsbHLH46	Maker00026766	Chr12 (5086087..5087439)	Nuclear	5.20	37837.62	335	-0.537	60.86	73.64
TsbHLH47	Maker00000467	Chr12 (6876629..6877750)	Nuclear	6.09	36650.59	321	-0.272	54.5	80.5
TsbHLH48	Maker00026481	Chr12 (878213..879614)	Nuclear	5.56	39298.77	348	-0.805	49.71	63.3
TsbHLH49	Maker00028535	Chr12 (14200693..14201660)	Nuclear	5.81	27113.57	239	-0.703	60.03	73.85
TsbHLH50	Maker00023442	Chr13 (884608..887695)	Extracellular	6.23	35461.45	325	-0.296	63.2	81.6
TsbHLH51	Maker00032793	Chr13 (13613555..13615408)	Nuclear	6.28	38238.00	346	-0.586	66.41	80.66
TsbHLH52	Maker00026079	Chr13 (15133003..15136633)	Nuclear	5.34	37562.83	336	-0.775	54.67	71.96
TsbHLH53	Maker00025766	Chr13 (18252417..18255239)	Nuclear	5.71	52424.33	461	-0.566	52.17	86.25
TsbHLH54	Maker00025736	Chr13 (19956865..19957924)	Nuclear	9.85	20070.89	182	-0.826	51.33	73.41
TsbHLH55	Maker00025972	Chr13 (20574422..20576703)	Nuclear	7.69	49108.99	443	-0.815	44.62	49.1
TsbHLH56	Maker00010886	Chr14 (368015..370238)	Nuclear	8.52	47084.03	426	-0.785	50.72	54.72
TsbHLH57	Maker00010812	Chr14 (956193..957411)	Nuclear	9.44	25727.38	231	-0.667	57.91	72.64
TsbHLH58	Maker00017826	Chr14 (3009579..3012188)	Nuclear	6.49	51750.12	457	-0.507	54.99	87.24
TsbHLH59	Maker00031652	Chr14 (5554749..5558337)	Nuclear	5.63	38256.58	343	-0.794	52.85	70.5
TsbHLH60	Maker00020111	Chr14 (6979796..6981643)	Nuclear	6.08	38340.11	346	-0.545	61.04	84.05
TsbHLH61	Maker00003238	Chr14 (19663257..19664632)	Nuclear	6.45	27267.72	240	-0.567	54.94	71.88
TsbHLH62	Maker00029664	Chr15 (566470..569209)	Extracellular	6.06	80535.86	743	-0.523	49.75	66.12
TsbHLH63	Maker00027153	Chr15 (18003406..18004337)	Nuclear	9.33	29072.05	260	-0.434	53.92	79.85
TsbHLH64	Maker00027898	Chr15 (19929964..19934220)	Nuclear	6.60	30816.08	288	-0.342	57.73	73.3
TsbHLH65	Maker00027975	Chr15 (20723381..20724599)	Nuclear	5.24	38405.70	342	-0.606	62.72	72.4
TsbHLH66	Maker00009553	Chr16 (793052..794268)	Nuclear	5.37	38481.68	343	-0.655	55.45	70.2

Table S2. (Cont'd.).

Gene name	Gene locus	Chromosome location	Subcellular localization	pI	Mw (Da)	Protein length	GRAVY	Instability index	Aliphatic index
TsbHLH67	Maker00009350	Chr16 (1488262..1492840)	Nuclear	5.59	35460.92	330	-0.437	59.67	72.21
TsbHLH68	Maker00015803	Chr16 (23020557..23023400)	Extracellular	6.34	78479.25	719	-0.617	50.69	58.28
TsbHLH69	Maker00024125	Chr17 (11484413..11504232)	Extracellular	9.54	67233.55	603	-0.52	46.29	81.33
TsbHLH70	Maker00015881	Chr17 (11768005..11787095)	Extracellular	9.57	64379.42	576	-0.513	46.4	82.24
TsbHLH71	Maker00025436	Chr17 (22355049..22357034)	Nuclear	6.16	46170.16	410	-0.968	61.19	56.2
TsbHLH72	Maker00007199	Chr18(14004822..14005834)	Nuclear	9.62	27924.00	249	-0.392	53.62	88.39
TsbHLH73	Maker00007206	Chr18 (14097667..14098722)	Nuclear	8.85	21510.44	193	-0.601	45.83	81.87
TsbHLH74	Maker00024052	Chr19 (295410..296849)	Nuclear	6.44	54128.10	479	-0.472	40	77.24
TsbHLH75	Maker00002708	Chr19 (1550213..1553479)	Nuclear	5.29	71449.79	637	-0.4	48.68	88.45
TsbHLH76	Maker00003008	Chr19 (1834115..1835210)	Nuclear	5.80	25141.36	225	-0.624	57.59	84.13
TsbHLH77	Maker00000145	Chr19 (17552093..17557534)	Nuclear	8.78	61819.65	563	-0.894	51.11	59.77
TsbHLH78	Maker00031247	Chr20 (6637178..6642650)	Nuclear	8.67	60979.60	555	-0.862	54.72	60.81
TsbHLH79	Maker00015674	Chr20 (9820381..9822745)	Extracellular	9.24	44247.22	400	-0.621	64.62	73.42
TsbHLH80	Maker00017436	Chr20 (20143530..20146781)	Nuclear	5.59	70314.82	628	-0.379	51.63	88.77
TsbHLH81	Maker00022216	Chr20 (21532607..21534052)	Nuclear	5.80	54397.39	481	-0.483	40.19	78.36
TsbHLH82	Maker00005326	Chr21 (2160349..2161833)	Nuclear	8.67	21855.44	194	-0.059	55.62	109.9
TsbHLH83	Maker00012386	Chr21 (4224365..4225254)	Nuclear	9.31	28406.41	245	-0.782	58.68	69.27
TsbHLH84	Maker00012266	Chr21 (4369289..4370190)	Nuclear	9.53	28918.00	249	-0.755	59.33	70.48
TsbHLH85	Maker00012332	Chr21 (7637834..7639273)	Nuclear	5.30	47876.40	424	-0.468	61.99	80.02
TsbHLH86	Maker00020218	Chr21 (13015607..13021623)	Nuclear	8.18	38242.99	355	-0.621	52.83	58.79
TsbHLH87	Maker00001640	Chr22 (12853267..12854837)	Nuclear	5.43	47747.65	424	-0.605	63.32	76.34
TsbHLH88	Maker00006644	Chr22 (16360159..16361034)	Nuclear	7.67	26696.24	229	-0.81	58.64	74.5
TsbHLH89	Maker00006506	Chr22 (17527030..17528542)	Nuclear	8.32	22490.13	201	-0.03	54.76	107.56
TsbHLH90	Maker00020960	Chr23 (3834030..3837402)	Nuclear	5.55	50708.20	461	-0.444	48.52	77.27
TsbHLH91	Maker00030964	Chr23 (7582938..7585862)	Extracellular	7.18	63318.75	572	-0.693	53.02	56.05
TsbHLH92	Maker00005769	Chr23 (11911712..11913730)	Nuclear	5.33	64508.77	589	-0.626	53.78	66.76
TsbHLH93	Maker00032146	Chr23 (12136352..12138367)	Nuclear	5.40	73740.81	671	-0.662	52.85	66.15
TsbHLH94	Maker00032129	Chr23 (12646089..12648200)	Nuclear	8.75	35998.78	320	-0.456	54.85	88.97
TsbHLH95	Maker00030534	Chr23 (21661017..21666382)	Nuclear	6.12	54922.97	502	-0.612	61.01	58.51
TsbHLH96	Maker00021340	Chr23 (21910003..21915499)	Nuclear	5.81	63000.32	578	-0.448	55.21	65.14
TsbHLH97	Maker00001126	Chr23 (24205967..24207694)	Nuclear	6.06	55464.15	503	-0.511	46.33	73.4
TsbHLH98	Maker00018792	Chr23 (25744972..25750094)	Nuclear	5.26	76404.19	683	-0.675	65.32	73.07
TsbHLH99	Maker00014851	Chr23 (28041582..28044050)	Extracellular	9.70	70444.27	632	-0.69	59.61	65.73
TsbHLH100	Maker00014721	Chr23 (28421204..28427214)	Extracellular	5.84	89708.14	797	-0.273	48.63	94.42
TsbHLH101	Maker00014629	Chr23 (28555453..28556928)	Nuclear	5.85	54580.51	491	-0.465	46.1	80.59
TsbHLH102	Maker00014854	Chr23 (28813565..28815412)	Nuclear	6.14	68201.79	615	-0.455	44.41	80.05
TsbHLH103	Maker00029181	Chr23 (31344255..31347502)	Nuclear	8.35	50644.10	462	-0.675	57.53	51.8
TsbHLH104	Maker00023868	Chr24 (34907..36601)	Nuclear	5.36	51382.22	458	-0.602	47.24	80.87
TsbHLH105	Maker00023851	Chr24 (817898..821067)	Nuclear	8.36	50786.27	469	-0.606	56.68	54.8
TsbHLH106	Maker00022912	Chr24 (2835979..2837826)	Nuclear	6.04	68491.05	615	-0.457	43.47	79.24
TsbHLH107	Maker00022913	Chr24 (3167947..3169422)	Nuclear	5.58	54693.69	491	-0.469	48.11	81.38
TsbHLH108	Maker00022717	Chr24 (3477314..3478379)	Nuclear	9.62	23541.03	207	-0.431	56.51	88.5
TsbHLH109	Maker00022716	Chr24 (6572879..6577774)	Nuclear	5.51	76383.28	684	-0.662	62.91	70.13
TsbHLH110	Maker00012648	Chr24 (8425028..8426545)	Nuclear	6.18	55664.86	505	-0.41	46.51	80.08
TsbHLH111	Maker00000517	Chr24(11349277..11355169)	Nuclear	6.27	64417.39	589	-0.622	59.18	56.01
TsbHLH112	Maker00028131	Chr24 (19742445..19744042)	Nuclear	9.62	38069.60	331	-0.461	57.98	88.67
TsbHLH113	Maker00028128	Chr24 (20108914..20110937)	Nuclear	5.55	73266.36	667	-0.679	52.13	66.82
TsbHLH114	Maker00033429	Chr24 (23460628..23463581)	Extracellular	7.97	63340.83	573	-0.727	57.89	53.6
TsbHLH115	Maker00012989	Chr24 (27270898..27274255)	Nuclear	5.74	50589.12	458	-0.452	49.95	78.41
TsbHLH116	Maker00013337	Chr24 (27843710..27845103)	Nuclear	8.91	29975.10	268	-0.462	57.14	83.28
TsbHLH117	Maker00015635	Chr25 (665432..667880)	Extracellular	5.99	49462.87	471	-0.55	43.72	65.73
TsbHLH118	Maker00011332	Chr25(4243911..4244880)	Nuclear	5.22	25603.01	222	-0.532	61.48	79.5
TsbHLH119	Maker00019989	Chr25 (15151423..15153720)	Nuclear	9.17	58204.07	520	-0.345	67.06	86.67
TsbHLH120	Maker00025619	Chr26 (6970025..6972647)	Nuclear	9.34	54454.21	489	-0.226	66.76	91.17
TsbHLH121	Maker00016443	Chr26 (7058058..7060190)	Nuclear	9.27	53052.54	475	-0.27	68.26	89.54
TsbHLH122	Maker00033771	Chr26 (18749485..18750474)	Nuclear	5.25	17041.27	149	-0.33	58.44	91.07
TsbHLH123	Maker00021458	Chr27 (8285174..8287218)	Nuclear	6.48	33373.19	302	-0.912	58.04	59.8
TsbHLH124	Maker00014264	Chr27 (17958109..17960342)	Nuclear	5.49	35000.06	319	-0.713	62.48	59.06
TsbHLH125	Maker00003833	Chr27 (20970197..20971581)	Nuclear	5.20	39047.94	361	-0.756	52.42	64.1
TsbHLH126	Maker00003830	Chr27 (21705727..21708176)	Nuclear	9.15	38421.82	342	-0.48	39.3	72.69
TsbHLH127	Maker00003865	Chr27 (22133992..22136580)	Nuclear	5.47	65242.71	573	-0.671	44.23	76.81
TsbHLH128	Maker00033158	Chr28 (1423928..1425207)	Nuclear	7.73	37474.78	336	-0.379	46.92	80.09
TsbHLH129	Maker00010164	Chr28 (2042005..2043594)	Nuclear	5.34	42580.95	391	-0.74	57.59	63.91
TsbHLH130	Maker00010118	Chr28 (2972056..2974577)	Extracellular	6.14	26131.05	240	-0.693	47.42	65.04
TsbHLH131	Maker00009959	Chr28 (4598589..4600722)	Nuclear	6.14	28014.26	251	-0.781	61.92	60.28
TsbHLH132	Maker00028576	Chr28 (8172882..8174915)	Nuclear	6.86	33445.37	302	-0.903	58.57	61.69

Table S3. Correlation analysis of *TsbHLHs* and terpenoid synthesis genes.

		TsbHLH7	TsbHLH8	TsbHLH13	TsbHLH15	TsbHLH24	TsbHLH29	TsbHLH30	TsbHLH33	TsbHLH39	TsbHLH43
TsbHLH7	Pearson correlation coefficient	1	0.843	-0.068	0.935	-0.777	-0.096	0.654	-0.837	0.047	0.568
	Sig. (2-tailed)		0.157	0.932	0.065	0.223	0.904	0.346	0.163	0.953	0.432
TsbHLH8	Pearson correlation coefficient	0.843	1	-0.556	0.705	-0.378	-0.467	0.916	-0.617	0.083	0.868
	Sig. (2-tailed)	0.157		0.444	0.295	0.622	0.533	0.084	0.383	0.917	0.132
TsbHLH13	Pearson correlation coefficient	-0.068	-0.556	1	0.197	-0.558	0.924	-0.552	-0.286	-0.441	-0.569
	Sig. (2-tailed)	0.932	0.444		0.803	0.442	0.076	0.448	0.714	0.559	0.431
TsbHLH15	Pearson correlation coefficient	0.935	0.705	0.197	1	-0.921	0.241	0.613	-0.974	-0.286	0.544
	Sig. (2-tailed)	0.065	0.295	0.803		0.079	0.759	0.387	0.026	0.714	0.456
TsbHLH24	Pearson correlation coefficient	-0.777	-0.378	-0.558	-0.921	1	-0.545	-0.279	0.923	0.365	-0.209
	Sig. (2-tailed)	0.223	0.622	0.442	0.079		0.455	0.721	0.077	0.635	0.791
TsbHLH29	Pearson correlation coefficient	-0.096	-0.467	0.924	0.241	-0.545	1	-0.319	-0.398	-0.749	-0.305
	Sig. (2-tailed)	0.904	0.533	0.076	0.759	0.455		0.681	0.602	0.251	0.695
TsbHLH30	Pearson correlation coefficient	0.654	0.916	-0.552	0.613	-0.279	-0.319	1	-0.611	-0.248	0.994
	Sig. (2-tailed)	0.346	0.084	0.448	0.387	0.721	0.681		0.389	0.752	0.006
TsbHLH33	Pearson correlation coefficient	-0.837	-0.617	-0.286	-0.974	0.923	-0.398	-0.611	1	0.494	-0.561
	Sig. (2-tailed)	0.163	0.383	0.714	0.026	0.077	0.602	0.389		0.506	0.439
TsbHLH39	Pearson correlation coefficient	0.047	0.083	-0.441	-0.286	0.365	-0.749	-0.248	0.494	1	-0.304
	Sig. (2-tailed)	0.953	0.917	0.559	0.714	0.635	0.251	0.752	0.506		0.696
TsbHLH43	Pearson correlation coefficient	0.568	0.868	-0.569	0.544	-0.209	-0.305	0.994	-0.561	-0.304	1
	Sig. (2-tailed)	0.432	0.132	0.431	0.456	0.791	0.695	0.006	0.439	0.696	
TsbHLH71	Pearson correlation coefficient	0.708	0.849	-0.29	0.759	-0.5	-0.039	0.958	-0.792	-0.455	0.948
	Sig. (2-tailed)	0.292	0.151	0.71	0.241	0.5	0.961	0.042	0.208	0.545	0.052
TsbHLH75	Pearson correlation coefficient	-0.186	-0.492	0.868	0.165	-0.451	0.989	-0.29	-0.343	-0.815	-0.26
	Sig. (2-tailed)	0.814	0.508	0.132	0.835	0.549	0.011	0.71	0.657	0.185	0.74
TsbHLH91	Pearson correlation coefficient	-0.108	-0.524	0.967	0.21	-0.542	0.991	-0.421	-0.346	-0.652	-0.416
	Sig. (2-tailed)	0.892	0.476	0.033	0.79	0.458	0.009	0.579	0.654	0.348	0.584
TsbHLH94	Pearson correlation coefficient	0.536	0.029	0.806	0.72	-0.933	0.724	-0.081	-0.737	-0.342	-0.146
	Sig. (2-tailed)	0.464	0.971	0.194	0.28	0.067	0.276	0.919	0.263	0.658	0.854
TsbHLH97	Pearson correlation coefficient	0.772	0.636	0.205	0.929	-0.843	0.384	0.698	-0.982	-0.598	0.666
	Sig. (2-tailed)	0.228	0.364	0.795	0.071	0.157	0.616	0.302	0.018	0.402	0.334
TsbHLH103	Pearson correlation coefficient	0.211	-0.344	0.927	0.382	-0.704	0.751	-0.485	-0.392	-0.176	-0.542
	Sig. (2-tailed)	0.789	0.656	0.073	0.618	0.296	0.249	0.515	0.608	0.824	0.458
TsbHLH108	Pearson correlation coefficient	0.554	0.037	0.789	0.715	-0.926	0.678	-0.105	-0.714	-0.265	-0.176
	Sig. (2-tailed)	0.446	0.963	0.211	0.285	0.074	0.322	0.895	0.286	0.735	0.824
TsbHLH112	Pearson correlation coefficient	0.829	0.411	0.383	0.806	-0.862	0.194	0.124	-0.697	0.156	0.019
	Sig. (2-tailed)	0.171	0.589	0.617	0.194	0.138	0.806	0.876	0.303	0.844	0.981
TsbHLH124	Pearson correlation coefficient	0.185	-0.37	0.865	0.297	-0.617	0.624	-0.572	-0.27	0.016	-0.638
	Sig. (2-tailed)	0.815	0.63	0.135	0.703	0.383	0.376	0.428	0.73	0.984	0.362

Table S3. (Cont'd.).

		TsbHLH7	TsbHLH8	TsbHLH13	TsbHLH15	TsbHLH24	TsbHLH29	TsbHLH30	TsbHLH33	TsbHLH39	TsbHLH43
TsbHLH131	Pearson correlation coefficient	0.305	-0.251	0.901	0.469	-0.767	0.732	-0.402	-0.472	-0.182	-0.464
	Sig. (2-tailed)	0.695	0.749	0.099	0.531	0.233	0.268	0.598	0.528	0.818	0.536
TsAACT	Pearson correlation coefficient	-0.52	-0.841	0.88	-0.239	-0.131	0.871	-0.71	0.098	-0.494	-0.677
	Sig. (2-tailed)	0.48	0.159	0.12	0.761	0.869	0.129	0.29	0.902	0.506	0.323
TsDXR	Pearson correlation coefficient	0.226	-0.333	0.891	0.364	-0.68	0.681	-0.511	-0.352	-0.073	-0.575
	Sig. (2-tailed)	0.774	0.667	0.109	0.636	0.32	0.319	0.489	0.648	0.927	0.425
TsDXS	Pearson correlation coefficient	0.301	-0.222	0.931	0.532	-0.819	0.852	-0.284	-0.583	-0.413	-0.33
	Sig. (2-tailed)	0.699	0.778	0.069	0.468	0.181	0.148	0.716	0.417	0.587	0.67
TsFPPS1	Pearson correlation coefficient	0.553	0.627	-0.598	0.223	0.005	-0.804	0.303	-0.007	0.825	0.226
	Sig. (2-tailed)	0.447	0.373	0.402	0.777	0.995	0.196	0.697	0.993	0.175	0.774
TsGGPPS	Pearson correlation coefficient	-0.085	-0.118	0.447	0.251	-0.336	0.754	0.219	-0.462	-0.999	0.278
	Sig. (2-tailed)	0.915	0.882	0.553	0.749	0.664	0.246	0.781	0.538	0.001	0.722
TsGPPS1	Pearson correlation coefficient	0.734	0.441	0.957	0.474	-0.955	0.576	0.454	-0.978	-0.582	0.409
	Sig. (2-tailed)	0.266	0.559	0.043	0.526	0.045	0.424	0.546	0.022	0.418	0.591
TsHMGR	Pearson correlation coefficient	-0.768	-0.772	0.485	-0.491	0.261	0.652	-0.46	0.292	-0.65	-0.371
	Sig. (2-tailed)	0.232	0.228	0.515	0.509	0.739	0.348	0.54	0.708	0.35	0.629
TsMTPS	Pearson correlation coefficient	-0.387	-0.614	0.797	-0.039	-0.246	0.939	-0.365	-0.156	-0.809	-0.314
	Sig. (2-tailed)	0.613	0.386	0.203	0.961	0.754	0.061	0.635	0.844	0.191	0.686
TsHMGS	Pearson correlation coefficient	-0.332	0.227	-0.852	-0.455	0.743	-0.642	0.424	0.43	0.057	0.496
	Sig. (2-tailed)	0.668	0.773	0.148	0.545	0.257	0.358	0.576	0.57	0.943	0.504
TsIDI	Pearson correlation coefficient	-0.279	-0.403	0.64	0.078	-0.272	0.877	-0.09	-0.293	-0.943	-0.029
	Sig. (2-tailed)	0.721	0.597	0.36	0.922	0.728	0.123	0.91	0.707	0.057	0.971
TsFPPS2	Pearson correlation coefficient	0.221	-0.227	0.48	0.133	-0.351	0.116	-0.578	0.003	0.546	-0.666
	Sig. (2-tailed)	0.779	0.773	0.52	0.867	0.649	0.884	0.422	0.997	0.454	0.334
TsMDS	Pearson correlation coefficient	-0.007	-0.457	0.581	-0.051	-0.231	0.227	-0.756	0.153	0.474	-0.824
	Sig. (2-tailed)	0.993	0.543	0.419	0.949	0.769	0.773	0.244	0.847	0.526	0.176
TsMVD	Pearson correlation coefficient	0.237	-0.18	0.398	0.118	-0.308	0.025	-0.547	0.034	0.617	-0.638
	Sig. (2-tailed)	0.763	0.82	0.602	0.882	0.692	0.975	0.453	0.966	0.383	0.362
TsTPS28	Pearson correlation coefficient	0.392	-0.054	0.429	0.293	-0.466	0.079	-0.423	-0.144	0.534	-0.522
	Sig. (2-tailed)	0.608	0.946	0.571	0.707	0.534	0.921	0.577	0.856	0.466	0.478
TsGPPS2	Pearson correlation coefficient	0.525	0.15	0.231	0.366	-0.452	-0.112	-0.245	-0.186	0.633	-0.352
	Sig. (2-tailed)	0.475	0.85	0.769	0.634	0.548	0.888	0.755	0.814	0.367	0.648
TsHDR	Pearson correlation coefficient	0.228	-0.287	0.955	0.476	-0.778	0.887	-0.326	-0.54	-0.449	-0.365
	Sig. (2-tailed)	0.772	0.713	0.045	0.524	0.222	0.113	0.674	0.46	0.551	0.635
TsHDS	Pearson correlation coefficient	-0.058	-0.585	0.932	0.101	-0.471	0.724	-0.714	-0.117	-0.087	-0.755
	Sig. (2-tailed)	0.942	0.415	0.068	0.899	0.529	0.276	0.286	0.883	0.913	0.245

Table S3. (Cont'd.).

		TsbHLH71	TsbHLH75	TsbHLH91	TsbHLH94	TsbHLH97	TsbHLH103	TsbHLH108	TsbHLH112	TsbHLH124
TsbHLH7	Pearson correlation coefficient	0.708	-0.186	-0.108	0.536	0.772	0.211	0.554	0.829	0.185
	Sig. (2-tailed)	0.292	0.814	0.892	0.464	0.228	0.789	0.446	0.171	0.815
TsbHLH8	Pearson correlation coefficient	0.849	-0.492	-0.524	0.029	0.636	-0.344	0.037	0.411	-0.37
	Sig. (2-tailed)	0.151	0.508	0.476	0.971	0.364	0.656	0.963	0.589	0.63
TsbHLH13	Pearson correlation coefficient	-0.29	0.868	0.967	0.806	0.205	0.927	0.789	0.383	0.865
	Sig. (2-tailed)	0.71	0.132	0.033	0.194	0.795	0.073	0.211	0.617	0.135
TsbHLH15	Pearson correlation coefficient	0.759	0.165	0.21	0.72	0.929	0.382	0.715	0.806	0.297
	Sig. (2-tailed)	0.241	0.835	0.79	0.28	0.071	0.618	0.285	0.194	0.703
TsbHLH24	Pearson correlation coefficient	-0.5	-0.451	-0.542	-0.933	-0.843	-0.704	-0.926	-0.862	-0.617
	Sig. (2-tailed)	0.5	0.549	0.458	0.067	0.157	0.296	0.074	0.138	0.383
TsbHLH29	Pearson correlation coefficient	-0.039	0.989	0.991	0.724	0.384	0.751	0.678	0.194	0.624
	Sig. (2-tailed)	0.961	0.011	0.009	0.276	0.616	0.249	0.322	0.806	0.376
TsbHLH30	Pearson correlation coefficient	0.958	-0.29	-0.421	-0.081	0.698	-0.485	-0.105	0.124	-0.572
	Sig. (2-tailed)	0.042	0.71	0.579	0.919	0.302	0.515	0.895	0.876	0.428
TsbHLH33	Pearson correlation coefficient	-0.792	-0.343	-0.346	-0.737	-0.982	-0.392	-0.714	-0.697	-0.27
	Sig. (2-tailed)	0.208	0.657	0.654	0.263	0.018	0.608	0.286	0.303	0.73
TsbHLH39	Pearson correlation coefficient	-0.455	-0.815	-0.652	-0.342	-0.598	-0.176	-0.265	0.156	0.016
	Sig. (2-tailed)	0.545	0.185	0.348	0.658	0.402	0.824	0.735	0.844	0.984
TsbHLH43	Pearson correlation coefficient	0.948	-0.26	-0.416	-0.146	0.666	-0.542	-0.176	0.019	-0.638
	Sig. (2-tailed)	0.052	0.74	0.584	0.854	0.334	0.458	0.824	0.981	0.362
TsbHLH71	Pearson correlation coefficient	1	-0.022	-0.145	0.173	0.869	-0.248	0.138	0.251	-0.373
	Sig. (2-tailed)		0.978	0.855	0.827	0.131	0.752	0.862	0.749	0.627
TsbHLH75	Pearson correlation coefficient	-0.022	1	0.965	0.623	0.356	0.648	0.569	0.058	0.509
	Sig. (2-tailed)	0.978		0.035	0.377	0.644	0.352	0.431	0.942	0.491
TsbHLH91	Pearson correlation coefficient	-0.145	0.965	1	0.753	0.31	0.822	0.717	0.247	0.717
	Sig. (2-tailed)	0.855	0.035		0.247	0.69	0.178	0.283	0.753	0.283
TsbHLH94	Pearson correlation coefficient	0.173	0.623	0.753	1	0.63	0.911	0.997	0.817	0.843
	Sig. (2-tailed)	0.827	0.377	0.247		0.37	0.089	0.003	0.183	0.157
TsbHLH97	Pearson correlation coefficient	0.869	0.356	0.31	0.63	1	0.259	0.595	0.552	0.115
	Sig. (2-tailed)	0.131	0.644	0.69	0.37		0.741	0.405	0.448	0.885
TsbHLH103	Pearson correlation coefficient	-0.248	0.648	0.822	0.911	0.259	1	0.919	0.678	0.981
	Sig. (2-tailed)	0.752	0.352	0.178	0.089	0.741		0.081	0.322	0.019
TsbHLH108	Pearson correlation coefficient	0.138	0.569	0.717	0.997	0.595	0.919	1	0.852	0.867
	Sig. (2-tailed)	0.862	0.431	0.283	0.003	0.405	0.081		0.148	0.133
TsbHLH112	Pearson correlation coefficient	0.251	0.058	0.247	0.817	0.552	0.678	0.852	1	0.692
	Sig. (2-tailed)	0.749	0.942	0.753	0.183	0.448	0.322	0.148		0.308
TsbHLH124	Pearson correlation coefficient	-0.373	0.509	0.717	0.843	0.115	0.981	0.867	0.692	1
	Sig. (2-tailed)	0.627	0.491	0.283	0.157	0.885	0.019	0.133	0.308	

Table S3. (Cont'd.).

		TsbHLH71	TsbHLH75	TsbHLH91	TsbHLH94	TsbHLH97	TsbHLH103	TsbHLH108	TsbHLH112	TsbHLH124
TsbHLH131	Pearson correlation coefficient	-0.163	0.624	0.798	0.944	0.338	0.995	0.953	0.739	0.971
	Sig. (2-tailed)	0.837	0.376	0.202	0.056	0.662	0.005	0.047	0.261	0.029
TsAACT	Pearson correlation coefficient	-0.502	0.876	0.899	0.436	-0.119	0.662	0.404	-0.096	0.6
	Sig. (2-tailed)	0.498	0.124	0.101	0.564	0.881	0.338	0.596	0.904	0.4
TsDXR	Pearson correlation coefficient	-0.293	0.569	0.762	0.89	0.205	0.995	0.907	0.709	0.995
	Sig. (2-tailed)	0.707	0.431	0.238	0.11	0.795	0.005	0.093	0.291	0.005
TsDXS	Pearson correlation coefficient	-0.012	0.767	0.888	0.966	0.484	0.961	0.956	0.666	0.89
	Sig. (2-tailed)	0.988	0.233	0.112	0.034	0.516	0.039	0.044	0.334	0.11
TsFPPS1	Pearson correlation coefficient	0.12	-0.879	-0.754	-0.175	-0.076	-0.257	-0.109	0.424	-0.121
	Sig. (2-tailed)	0.88	0.121	0.246	0.825	0.924	0.743	0.891	0.576	0.879
TsGGPPS	Pearson correlation coefficient	0.424	0.823	0.658	0.324	0.567	0.172	0.247	-0.185	-0.019
	Sig. (2-tailed)	0.576	0.177	0.342	0.676	0.433	0.828	0.753	0.815	0.981
TsGPPS1	Pearson correlation coefficient	0.678	0.52	0.533	0.835	0.952	0.54	0.807	0.691	0.409
	Sig. (2-tailed)	0.322	0.48	0.467	0.165	0.048	0.46	0.193	0.309	0.591
TsHMGR	Pearson correlation coefficient	-0.337	0.741	0.619	-0.047	-0.207	0.128	-0.104	-0.608	0.033
	Sig. (2-tailed)	0.663	0.259	0.381	0.953	0.793	0.872	0.896	0.392	0.967
TsMTPS	Pearson correlation coefficient	-0.128	0.976	0.911	0.442	0.193	0.519	0.384	-0.155	0.386
	Sig. (2-tailed)	0.872	0.024	0.089	0.558	0.807	0.481	0.616	0.845	0.614
TsHMGS	Pearson correlation coefficient	0.208	-0.523	-0.721	-0.919	-0.281	-0.986	-0.939	-0.781	-0.985
	Sig. (2-tailed)	0.792	0.477	0.279	0.081	0.719	0.014	0.061	0.219	0.015
TsIDI	Pearson correlation coefficient	0.136	0.936	0.811	0.373	0.371	0.342	0.301	-0.21	0.174
	Sig. (2-tailed)	0.864	0.064	0.189	0.627	0.629	0.658	0.699	0.79	0.826
TsFPPS2	Pearson correlation coefficient	-0.521	-0.018	0.244	0.54	-0.19	0.728	0.601	0.692	0.845
	Sig. (2-tailed)	0.479	0.982	0.756	0.46	0.81	0.272	0.399	0.308	0.155
TsMDS	Pearson correlation coefficient	-0.685	0.111	0.358	0.49	-0.328	0.755	0.544	0.532	0.867
	Sig. (2-tailed)	0.315	0.889	0.642	0.51	0.672	0.245	0.456	0.468	0.133
TsMVD	Pearson correlation coefficient	-0.515	-0.11	0.154	0.48	-0.22	0.665	0.546	0.683	0.794
	Sig. (2-tailed)	0.485	0.89	0.846	0.52	0.78	0.335	0.454	0.317	0.206
TsTPS28	Pearson correlation coefficient	-0.362	-0.064	0.198	0.599	-0.043	0.717	0.661	0.802	0.825
	Sig. (2-tailed)	0.638	0.936	0.802	0.401	0.957	0.283	0.339	0.198	0.175
TsGPPS2	Pearson correlation coefficient	-0.229	-0.256	-0.001	0.51	0.005	0.569	0.578	0.832	0.687
	Sig. (2-tailed)	0.771	0.744	0.999	0.49	0.995	0.431	0.422	0.168	0.313
TsHDR	Pearson correlation coefficient	-0.051	0.809	0.921	0.943	0.448	0.957	0.93	0.605	0.882
	Sig. (2-tailed)	0.949	0.191	0.079	0.057	0.552	0.043	0.07	0.395	0.118
TsHDS	Pearson correlation coefficient	-0.507	0.636	0.811	0.756	-0.015	0.958	0.768	0.487	0.966
	Sig. (2-tailed)	0.493	0.364	0.189	0.244	0.985	0.042	0.232	0.513	0.034

Table S3. (Cont'd.).

		TsbHLH131	TsAACT	TsDXR	TsDXS	TsFPPS1	TsGGPPS	TsGPPS1	TsHMGR	TsMTPS
TsbHLH7	Pearson correlation coefficient	0.305	-0.52	0.226	0.301	0.553	-0.085	0.734	-0.768	-0.387
	Sig. (2-tailed)	0.695	0.48	0.774	0.699	0.447	0.915	0.266	0.232	0.613
TsbHLH8	Pearson correlation coefficient	-0.251	-0.841	-0.333	-0.222	0.627	-0.118	0.441	-0.772	-0.614
	Sig. (2-tailed)	0.749	0.159	0.667	0.778	0.373	0.882	0.559	0.228	0.386
TsbHLH13	Pearson correlation coefficient	0.901	0.88	0.891	0.931	-0.598	0.447	0.474	0.485	0.797
	Sig. (2-tailed)	0.099	0.12	0.109	0.069	0.402	0.553	0.526	0.515	0.203
TsbHLH15	Pearson correlation coefficient	0.469	-0.239	0.364	0.532	0.223	0.251	0.927	-0.491	-0.039
	Sig. (2-tailed)	0.531	0.761	0.636	0.468	0.777	0.749	0.073	0.509	0.961
TsbHLH24	Pearson correlation coefficient	-0.767	-0.131	-0.68	-0.819	0.005	-0.336	-0.955	0.261	-0.246
	Sig. (2-tailed)	0.233	0.869	0.32	0.181	0.995	0.664	0.045	0.739	0.754
TsbHLH29	Pearson correlation coefficient	0.732	0.871	0.681	0.852	-0.804	0.754	0.576	0.652	0.939
	Sig. (2-tailed)	0.268	0.129	0.319	0.148	0.196	0.246	0.424	0.348	0.061
TsbHLH30	Pearson correlation coefficient	-0.402	-0.71	-0.511	-0.284	0.303	0.219	0.454	-0.46	-0.365
	Sig. (2-tailed)	0.598	0.29	0.489	0.716	0.697	0.781	0.546	0.54	0.635
TsbHLH33	Pearson correlation coefficient	-0.472	0.098	-0.352	-0.583	-0.007	-0.462	-0.978	0.292	-0.156
	Sig. (2-tailed)	0.528	0.902	0.648	0.417	0.993	0.538	0.022	0.708	0.844
TsbHLH39	Pearson correlation coefficient	-0.182	-0.494	-0.073	-0.413	0.825	-0.999	-0.582	-0.65	-0.809
	Sig. (2-tailed)	0.818	0.506	0.927	0.587	0.175	0.001	0.418	0.35	0.191
TsbHLH43	Pearson correlation coefficient	-0.464	-0.677	-0.575	-0.33	0.226	0.278	0.409	-0.371	-0.314
	Sig. (2-tailed)	0.536	0.323	0.425	0.67	0.774	0.722	0.591	0.629	0.686
TsbHLH71	Pearson correlation coefficient	-0.163	-0.502	-0.293	-0.012	0.12	0.424	0.678	-0.337	-0.128
	Sig. (2-tailed)	0.837	0.498	0.707	0.988	0.88	0.576	0.322	0.663	0.872
TsbHLH75	Pearson correlation coefficient	0.624	0.876	0.569	0.767	-0.879	0.823	0.52	0.741	0.976
	Sig. (2-tailed)	0.376	0.124	0.431	0.233	0.121	0.177	0.48	0.259	0.024
TsbHLH91	Pearson correlation coefficient	0.798	0.899	0.762	0.888	-0.754	0.658	0.533	0.619	0.911
	Sig. (2-tailed)	0.202	0.101	0.238	0.112	0.246	0.342	0.467	0.381	0.089
TsbHLH94	Pearson correlation coefficient	0.944	0.436	0.89	0.966	-0.175	0.324	0.835	-0.047	0.442
	Sig. (2-tailed)	0.056	0.564	0.11	0.034	0.825	0.676	0.165	0.953	0.558
TsbHLH97	Pearson correlation coefficient	0.338	-0.119	0.205	0.484	-0.076	0.567	0.952	-0.207	0.193
	Sig. (2-tailed)	0.662	0.881	0.795	0.516	0.924	0.433	0.048	0.793	0.807
TsbHLH103	Pearson correlation coefficient	0.995	0.662	0.995	0.961	-0.257	0.172	0.54	0.128	0.519
	Sig. (2-tailed)	0.005	0.338	0.005	0.039	0.743	0.828	0.46	0.872	0.481
TsbHLH108	Pearson correlation coefficient	0.953	0.404	0.907	0.956	-0.109	0.247	0.807	-0.104	0.384
	Sig. (2-tailed)	0.047	0.596	0.093	0.044	0.891	0.753	0.193	0.896	0.616
TsbHLH112	Pearson correlation coefficient	0.739	-0.096	0.709	0.666	0.424	-0.185	0.691	-0.608	-0.155
	Sig. (2-tailed)	0.261	0.904	0.291	0.334	0.576	0.815	0.309	0.392	0.845
TsbHLH124	Pearson correlation coefficient	0.971	0.6	0.995	0.89	-0.121	-0.019	0.409	0.033	0.386
	Sig. (2-tailed)	0.029	0.4	0.005	0.11	0.879	0.981	0.591	0.967	0.614

Table S3. (Cont'd.).

		TsbHLH131	**TsAACT**	**TsDXR**	**TsDXS**	**TsFPPS1**	**TsGGPPS**	**TsGPPS1**	**TsHMGR**	**TsMTPS**
TsbHLH131	Pearson correlation coefficient	1	0.598	0.99	0.97	-0.207	0.174	0.608	0.058	0.478
	Sig. (2-tailed)		0.402	0.01	0.03	0.793	0.826	0.392	0.942	0.522
TsAACT	Pearson correlation coefficient	0.598	1	0.614	0.652	-0.831	0.516	0.109	0.819	0.911
	Sig. (2-tailed)	0.402		0.386	0.348	0.169	0.484	0.891	0.181	0.089
TsDXR	Pearson correlation coefficient	0.99	0.614	1	0.931	-0.169	0.069	0.492	0.056	0.437
	Sig. (2-tailed)	0.01	0.386		0.069	0.831	0.931	0.508	0.944	0.563
TsDXS	Pearson correlation coefficient	0.97	0.652	0.931	1	-0.375	0.404	0.725	0.188	0.625
	Sig. (2-tailed)	0.03	0.348	0.069		0.625	0.596	0.275	0.812	0.375
TsFPPS1	Pearson correlation coefficient	-0.207	-0.831	-0.169	-0.375	1	-0.845	-0.153	-0.958	-0.958
	Sig. (2-tailed)	0.793	0.169	0.831	0.625		0.155	0.847	0.042	0.042
TsGGPPS	Pearson correlation coefficient	0.174	0.516	0.069	0.404	-0.845	1	0.554	0.678	0.824
	Sig. (2-tailed)	0.826	0.484	0.931	0.596	0.155		0.446	0.322	0.176
TsGPPS1	Pearson correlation coefficient	0.608	0.109	0.492	0.725	-0.153	0.554	1	-0.133	0.338
	Sig. (2-tailed)	0.392	0.891	0.508	0.275	0.847	0.446		0.867	0.662
TsHMGR	Pearson correlation coefficient	0.058	0.819	0.056	0.188	-0.958	0.678	-0.133	1	0.87
	Sig. (2-tailed)	0.942	0.181	0.944	0.812	0.042	0.322	0.867		0.13
TsMTPS	Pearson correlation coefficient	0.478	0.911	0.437	0.625	-0.958	0.824	0.338	0.87	1
	Sig. (2-tailed)	0.522	0.089	0.563	0.375	0.042	0.176	0.662	0.13	
TsHMGS	Pearson correlation coefficient	-0.992	-0.532	-0.994	-0.933	0.094	-0.049	-0.554	0.038	-0.373
	Sig. (2-tailed)	0.008	0.468	0.006	0.067	0.906	0.951	0.446	0.962	0.627
TsIDI	Pearson correlation coefficient	0.319	0.752	0.246	0.516	-0.954	0.952	0.437	0.829	0.957
	Sig. (2-tailed)	0.681	0.248	0.754	0.484	0.046	0.048	0.563	0.171	0.043
TsFPPS2	Pearson correlation coefficient	0.721	0.213	0.795	0.531	0.361	-0.55	0.061	-0.35	-0.126
	Sig. (2-tailed)	0.279	0.787	0.205	0.469	0.639	0.45	0.939	0.65	0.874
TsMDS	Pearson correlation coefficient	0.725	0.408	0.813	0.545	0.17	-0.468	-0.05	-0.125	0.043
	Sig. (2-tailed)	0.275	0.592	0.187	0.455	0.83	0.532	0.95	0.875	0.957
TsMVD	Pearson correlation coefficient	0.66	0.132	0.739	0.458	0.439	-0.621	0.014	-0.416	-0.214
	Sig. (2-tailed)	0.34	0.868	0.261	0.542	0.561	0.379	0.986	0.584	0.786
TsTPS28	Pearson correlation coefficient	0.727	0.096	0.784	0.546	0.452	-0.544	0.184	-0.479	-0.201
	Sig. (2-tailed)	0.273	0.904	0.216	0.454	0.548	0.456	0.816	0.521	0.799
TsGPPS2	Pearson correlation coefficient	0.595	-0.135	0.645	0.405	0.638	-0.648	0.178	-0.668	-0.404
	Sig. (2-tailed)	0.405	0.865	0.355	0.595	0.362	0.352	0.822	0.332	0.596
TsHDR	Pearson correlation coefficient	0.96	0.709	0.923	0.997	-0.442	0.443	0.694	0.264	0.681
	Sig. (2-tailed)	0.04	0.291	0.077	0.003	0.558	0.557	0.306	0.736	0.319
TsHDS	Pearson correlation coefficient	0.926	0.779	0.959	0.867	-0.332	0.093	0.29	0.278	0.559
	Sig. (2-tailed)	0.074	0.221	0.041	0.133	0.668	0.907	0.71	0.722	0.441

Table S3. (Cont'd.).

		TsHMGS	TsIDI	TsFPPS2	TsMDS	TsMVD	TsTPS28	TsGPPS2	TsHDR	TsHDS
TsbHLH7	Pearson correlation coefficient	-0.332	-0.279	0.221	-0.007	0.237	0.392	0.525	0.228	-0.058
	Sig. (2-tailed)	0.668	0.721	0.779	0.993	0.763	0.608	0.475	0.772	0.942
TsbHLH8	Pearson correlation coefficient	0.227	-0.403	-0.227	-0.457	-0.18	-0.054	0.15	-0.287	-0.585
	Sig. (2-tailed)	0.773	0.597	0.773	0.543	0.82	0.946	0.85	0.713	0.415
TsbHLH13	Pearson correlation coefficient	-0.852	0.64	0.48	0.581	0.398	0.429	0.231	0.955	0.932
	Sig. (2-tailed)	0.148	0.36	0.52	0.419	0.602	0.571	0.769	0.045	0.068
TsbHLH15	Pearson correlation coefficient	-0.455	0.078	0.133	-0.051	0.118	0.293	0.366	0.476	0.101
	Sig. (2-tailed)	0.545	0.922	0.867	0.949	0.882	0.707	0.634	0.524	0.899
TsbHLH24	Pearson correlation coefficient	0.743	-0.272	-0.351	-0.231	-0.308	-0.466	-0.452	-0.778	-0.471
	Sig. (2-tailed)	0.257	0.728	0.649	0.769	0.692	0.534	0.548	0.222	0.529
TsbHLH29	Pearson correlation coefficient	-0.642	0.877	0.116	0.227	0.025	0.079	-0.112	0.887	0.724
	Sig. (2-tailed)	0.358	0.123	0.884	0.773	0.975	0.921	0.888	0.113	0.276
TsbHLH30	Pearson correlation coefficient	0.424	-0.09	-0.578	-0.756	-0.547	-0.423	-0.245	-0.326	-0.714
	Sig. (2-tailed)	0.576	0.91	0.422	0.244	0.453	0.577	0.755	0.674	0.286
TsbHLH33	Pearson correlation coefficient	0.43	-0.293	0.003	0.153	0.034	-0.144	-0.186	-0.54	-0.117
	Sig. (2-tailed)	0.57	0.707	0.997	0.847	0.966	0.856	0.814	0.46	0.883
TsbHLH39	Pearson correlation coefficient	0.057	-0.943	0.546	0.474	0.617	0.534	0.633	-0.449	-0.087
	Sig. (2-tailed)	0.943	0.057	0.454	0.526	0.383	0.466	0.367	0.551	0.913
TsbHLH43	Pearson correlation coefficient	0.496	-0.029	-0.666	-0.824	-0.638	-0.522	-0.352	-0.365	-0.755
	Sig. (2-tailed)	0.504	0.971	0.334	0.176	0.362	0.478	0.648	0.635	0.245
TsbHLH71	Pearson correlation coefficient	0.208	0.136	-0.521	-0.685	-0.515	-0.362	-0.229	-0.051	-0.507
	Sig. (2-tailed)	0.792	0.864	0.479	0.315	0.485	0.638	0.771	0.949	0.493
TsbHLH75	Pearson correlation coefficient	-0.523	0.936	-0.018	0.111	-0.11	-0.064	-0.256	0.809	0.636
	Sig. (2-tailed)	0.477	0.064	0.982	0.889	0.89	0.936	0.744	0.191	0.364
TsbHLH91	Pearson correlation coefficient	-0.721	0.811	0.244	0.358	0.154	0.198	-0.001	0.921	0.811
	Sig. (2-tailed)	0.279	0.189	0.756	0.642	0.846	0.802	0.999	0.079	0.189
TsbHLH94	Pearson correlation coefficient	-0.919	0.373	0.54	0.49	0.48	0.599	0.51	0.943	0.756
	Sig. (2-tailed)	0.081	0.627	0.46	0.51	0.52	0.401	0.49	0.057	0.244
TsbHLH97	Pearson correlation coefficient	-0.281	0.371	-0.19	-0.328	-0.22	-0.043	0.005	0.448	-0.015
	Sig. (2-tailed)	0.719	0.629	0.81	0.672	0.78	0.957	0.995	0.552	0.985
TsbHLH103	Pearson correlation coefficient	-0.986	0.342	0.728	0.755	0.665	0.717	0.569	0.957	0.958
	Sig. (2-tailed)	0.014	0.658	0.272	0.245	0.335	0.283	0.431	0.043	0.042
TsbHLH108	Pearson correlation coefficient	-0.939	0.301	0.601	0.544	0.546	0.661	0.578	0.93	0.768
	Sig. (2-tailed)	0.061	0.699	0.399	0.456	0.454	0.339	0.422	0.07	0.232
TsbHLH112	Pearson correlation coefficient	-0.781	-0.21	0.692	0.532	0.683	0.802	0.832	0.605	0.487
	Sig. (2-tailed)	0.219	0.79	0.308	0.468	0.317	0.198	0.168	0.395	0.513
TsbHLH124	Pearson correlation coefficient	-0.985	0.174	0.845	0.867	0.794	0.825	0.687	0.882	0.966
	Sig. (2-tailed)	0.015	0.826	0.155	0.133	0.206	0.175	0.313	0.118	0.034

Table S3. (Cont'd.).

		TsHMGS	TsIDI	TsFPPS2	TsMDS	TsMVD	TsTPS28	TsGPPS2	TsHDR	TsHDS
TsbHLH131	Pearson correlation coefficient	-0.992	0.319	0.721	0.725	0.66	0.727	0.595	0.96	0.926
	Sig. (2-tailed)	0.008	0.681	0.279	0.275	0.34	0.273	0.405	0.04	0.074
TsAACT	Pearson correlation coefficient	-0.532	0.752	0.213	0.408	0.132	0.096	-0.135	0.709	0.779
	Sig. (2-tailed)	0.468	0.248	0.787	0.592	0.868	0.904	0.865	0.291	0.221
TsDXR	Pearson correlation coefficient	-0.994	0.246	0.795	0.813	0.739	0.784	0.645	0.923	0.959
	Sig. (2-tailed)	0.006	0.754	0.205	0.187	0.261	0.216	0.355	0.077	0.041
TsDXS	Pearson correlation coefficient	-0.933	0.516	0.531	0.545	0.458	0.546	0.405	0.997	0.867
	Sig. (2-tailed)	0.067	0.484	0.469	0.455	0.542	0.454	0.595	0.003	0.133
TsFPPS1	Pearson correlation coefficient	0.094	-0.954	0.361	0.17	0.439	0.452	0.638	-0.442	-0.332
	Sig. (2-tailed)	0.906	0.046	0.639	0.83	0.561	0.548	0.362	0.558	0.668
TsGGPPS	Pearson correlation coefficient	-0.049	0.952	-0.55	-0.468	-0.621	-0.544	-0.648	0.443	0.093
	Sig. (2-tailed)	0.951	0.048	0.45	0.532	0.379	0.456	0.352	0.557	0.907
TsGPPS1	Pearson correlation coefficient	-0.554	0.437	0.061	-0.05	0.014	0.184	0.178	0.694	0.29
	Sig. (2-tailed)	0.446	0.563	0.939	0.95	0.986	0.816	0.822	0.306	0.71
TsHMGR	Pearson correlation coefficient	0.038	0.829	-0.35	-0.125	-0.416	-0.479	-0.668	0.264	0.278
	Sig. (2-tailed)	0.962	0.171	0.65	0.875	0.584	0.521	0.332	0.736	0.722
TsMTPS	Pearson correlation coefficient	-0.373	0.957	-0.126	0.043	-0.214	-0.201	-0.404	0.681	0.559
	Sig. (2-tailed)	0.627	0.043	0.874	0.957	0.786	0.799	0.596	0.319	0.441
TsHMGS	Pearson correlation coefficient	1	-0.198	-0.8	-0.791	-0.748	-0.809	-0.69	-0.916	-0.922
	Sig. (2-tailed)		0.802	0.2	0.209	0.252	0.191	0.31	0.084	0.078
TsIDI	Pearson correlation coefficient	-0.198	1	-0.368	-0.231	-0.451	-0.409	-0.571	0.568	0.33
	Sig. (2-tailed)	0.802		0.632	0.769	0.549	0.591	0.429	0.432	0.67
TsFPPS2	Pearson correlation coefficient	-0.8	-0.368	1	0.97	0.996	0.984	0.927	0.502	0.752
	Sig. (2-tailed)	0.2	0.632		0.03	0.004	0.016	0.073	0.498	0.248
TsMDS	Pearson correlation coefficient	-0.791	-0.231	0.97	1	0.954	0.912	0.809	0.535	0.836
	Sig. (2-tailed)	0.209	0.769	0.03		0.046	0.088	0.191	0.465	0.164
TsMVD	Pearson correlation coefficient	-0.748	-0.451	0.996	0.954	1	0.984	0.945	0.426	0.69
	Sig. (2-tailed)	0.252	0.549	0.004	0.046		0.016	0.055	0.574	0.31
TsTPS28	Pearson correlation coefficient	-0.809	-0.409	0.984	0.912	0.984	1	0.973	0.505	0.691
	Sig. (2-tailed)	0.191	0.591	0.016	0.088	0.016		0.027	0.495	0.309
TsGPPS2	Pearson correlation coefficient	-0.69	-0.571	0.927	0.809	0.945	0.973	1	0.351	0.51
	Sig. (2-tailed)	0.31	0.429	0.073	0.191	0.055	0.027		0.649	0.49
TsHDR	Pearson correlation coefficient	-0.916	0.568	0.502	0.535	0.426	0.505	0.351	1	0.879
	Sig. (2-tailed)	0.084	0.432	0.498	0.465	0.574	0.495	0.649		0.121
TsHDS	Pearson correlation coefficient	-0.922	0.33	0.752	0.836	0.69	0.691	0.51	0.879	1
	Sig. (2-tailed)	0.078	0.67	0.248	0.164	0.31	0.309	0.49	0.121	